

## **5.1 Introduction**

Natural and synthetic quartz materials are widely used in application of archeological/geological dating and dosimetry based on their thermoluminescence (TL) and optically stimulated luminescence (OSL) studies. A large number of works has been done on bulk form (i.e. micron level of grain size) of synthetic quartz from many years. Current research work, on Nano phosphor material has great attraction due to its improved optical, electrical, mechanical and thermal properties. In present study efforts are made to understand the effect of the physical processes in Nano synthetic quartz on its TL and OSL properties. Based on the outcome of the findings efforts are being made to propose its use in dosimetric and dating applications. Nano Synthetic Quartz (NSQ) samples were prepared, chemically purified and used for the TL and OSL study under the influence of different physical conditions. The observed results of different experiments are discussed as below:

## **5.2 Thermoluminescence (TL) study of prepared NSQ samples**

Botter-Jensen L, McKeever S W S, Toktamis H et al. and Polymeris G et al. have done the significant work on thermoluminescence study of micron sized natural and synthetic quartz material<sup>1-4</sup>. The structure of TL outcomes; like shape of TL glow curve, TL glow peak position and TL intensity are studied under influence of physical treatments to the sample and experimental conditions. The changes in TL glow curve patterns depend upon magnitude of physical treatments like ionizing radiation, thermal treatment (fired temperature and annealing temperature), illumination of light, grain sizes, heating rate and other experimental conditions. Similarly, the physical treatments on synthetic and natural quartz leads to significant changes in TL outcomes which are widely used for retrospective dosimetry and archeological/geological dating applications<sup>1,2</sup>.

Past work on quartz have also reported that TL sensitivity is significantly changes in nano phosphors rather than micron sized phosphors<sup>5-7</sup>. Such changes in TL outcome of nano material established a correlation between TL signal and changes in optical properties of material at nano scale<sup>8-10</sup>.

Considering the facts and available literature, in present study we attempt to throw the light on thermoluminescence properties of NSQ material over

measurement temperature from 0°C to 398°C. Resultant outcomes of TL were studied under the influence of (i) beta dose(s) (ii) annealing temperature(s) (iii) optical bleaching temperature(s) (i.e. at room temperature and at elevated temperature-160°C). The TL results obtained under the influence of different proposed protocols were compared and the TL dose response curves (DRC) were recorded for predominantly contributed TL glow peaks and their DRC characteristics (sub-linear, linear and super-linear) were also considered.

### **5.2.1 Effect of beta dose on TL of un-annealed NSQ samples.**

The batches of unannealed NSQ samples were irradiated for different beta doses such as 48.03Gy, 81.43Gy, 120.83Gy, 160.23Gy and 199.63Gy. The TL glow curves of beta exposed samples were recorded from 0° to 398°C. The samples which were under the influence of 48.03Gy, 81.43Gy, 120.83Gy of beta dose showed two distinct TL glow peaks; a sharp one TL peak at 110°C and another broad TL peak at 300°C. The intensities of TL glow peaks at 110°C and 300°C increases from 74.8 counts to 142.2 counts and 54 counts to 129.4 counts respectively with the increase in dose. Further exposure of beta doses by 160.23Gy and 199.63Gy; it was also observed that the position of shallow 110°C TL glow peak was sustained with significant growth of TL counts, however under the influence of higher exposures; additional two new TL glow peaks were developed at 165°C and 220°C with the growth of TL counts by noticeable fading of 300°C TL glow peak. **(Fig. 5.1)**

It is well established that in TL mechanism, material must be previously irradiated so as to defects/traps are induced in the material. The lifetime of charges in the trap depend upon the strength of thermal treatment and is responsible for releasing of the electrons at adequate temperature. The growth of TL of NSQ specimens under present study is attributed to the rise in defect concentration due to increase in dose which increases the trapping probabilities of the electrons which corresponds to well defined of E<sub>1</sub>' centers<sup>11</sup>. The Electron Spin Resonance (ESR) study of NSQ sample also confirms the predominant development of E<sub>1</sub>' centre which is related to 110°C TL glow peak. ESR studies of quartz specimens also reveal that, either micron or nano sized quartz sample has similar color centers. Merely, the activity of

these centers under influence of optical stimulation may give significant results. Koul D K<sup>12</sup> has reported that typical glow peaks of natural quartz above the room temperature are 110°C, 230°C, 325°C and 375°C. Although 110°C TL glow peak is unstable at room temperature but it well worked in archaeology and retrospective dosimetry due to its pre-dose sensitization properties<sup>12</sup>. Pre-dose sensitization is a combined treatment of radiation and heat to the material. However, in present study, the 110°C TL glow peak was observed in NSQ sample exposed to beta radiations and only this beta dose sensitization in nano synthetic quartz is clearly discernible for the growth of TL peak.

The beta doses below 120.83Gy to unannealed NSQ samples in present studies contributed significantly to the growth of intensity and TL counts of traditional TL glow peak at 110°C and close to rapidly bleachable TL glow peak at 300°C. Beyond 120.83Gy of doses, the position of 110°C TL glow peak was sustained along with the development of two new TL glow peaks at 165°C and 220°C by fading of 300°C glow peak.

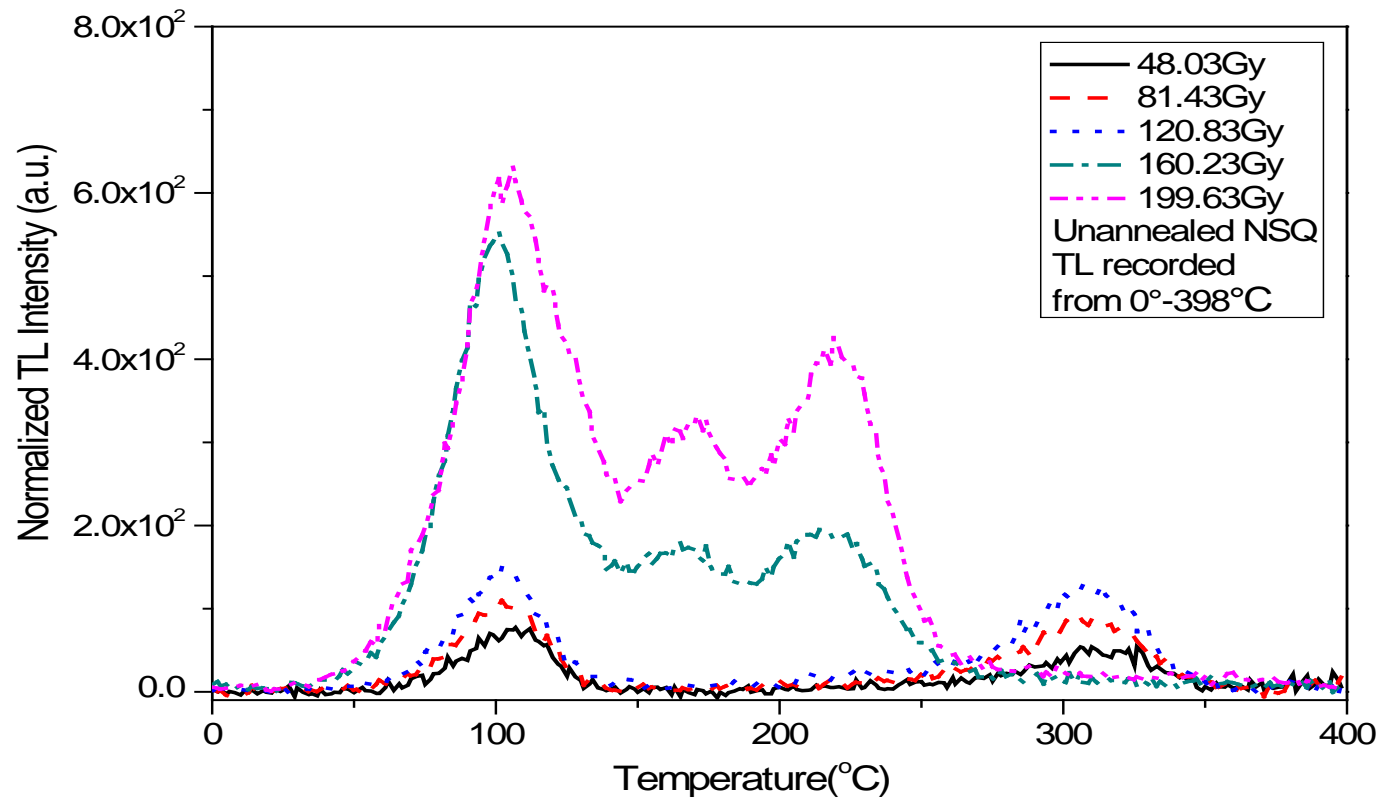


**Fig. 5.1** TL glow curve of unannealed NSQ for different beta doses.

## **2 Effect of beta dose on TL of annealed NSQ samples.**

To study the effect of annealing process on TL properties of NSQ material, the three different batches of samples were annealed at 400°C, 600°C and 1000°C for one hour duration. After completion of annealing treatment for definite duration, the samples were brought directly to the room temperature for quenching process. All three batches of thus annealed-quenched samples were exposed to 15.76Gy, 48.03Gy, 81.43Gy, 120.83Gy, 160.23Gy and 199.63Gy beta doses. The TL glow curves were recorded over the identical measurement temperature range. The specimens annealed at 400°C (**Fig. 5.2**) and 600°C (**Fig. 5.3**) followed by 15.76Gy, 48.03Gy, 81.43Gy, 120.83Gy beta doses showed the existence of typical shallow TL glow peak at 110°C along with development of wider span of new TL glow peaks between 220°C and 270°C. The TL intensity of 110°C glow peak increased from 432 counts to 8108.4 counts and from 61 counts to 3725.4 counts with increase in beta doses for the samples annealed at 400°C and 600°C respectively. The TL counts of 110°C TL glow peak further increased in the samples exposed to higher beta doses at 160.23Gy and 199.63Gy. Under influence of higher exposures, the position of 110°C TL glow peak was found to be indistinguishable. But the span of suggested new TL glow peak was scattered up to 300°C.

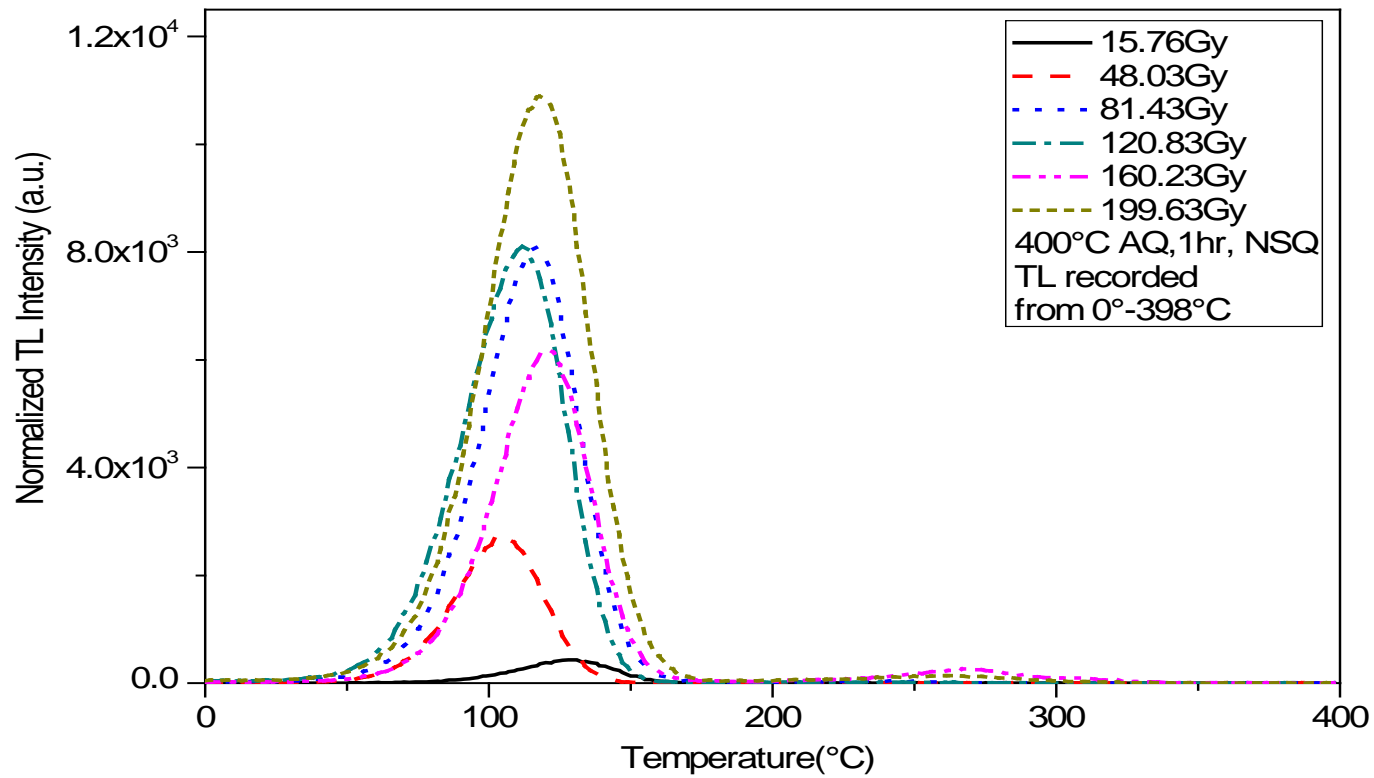
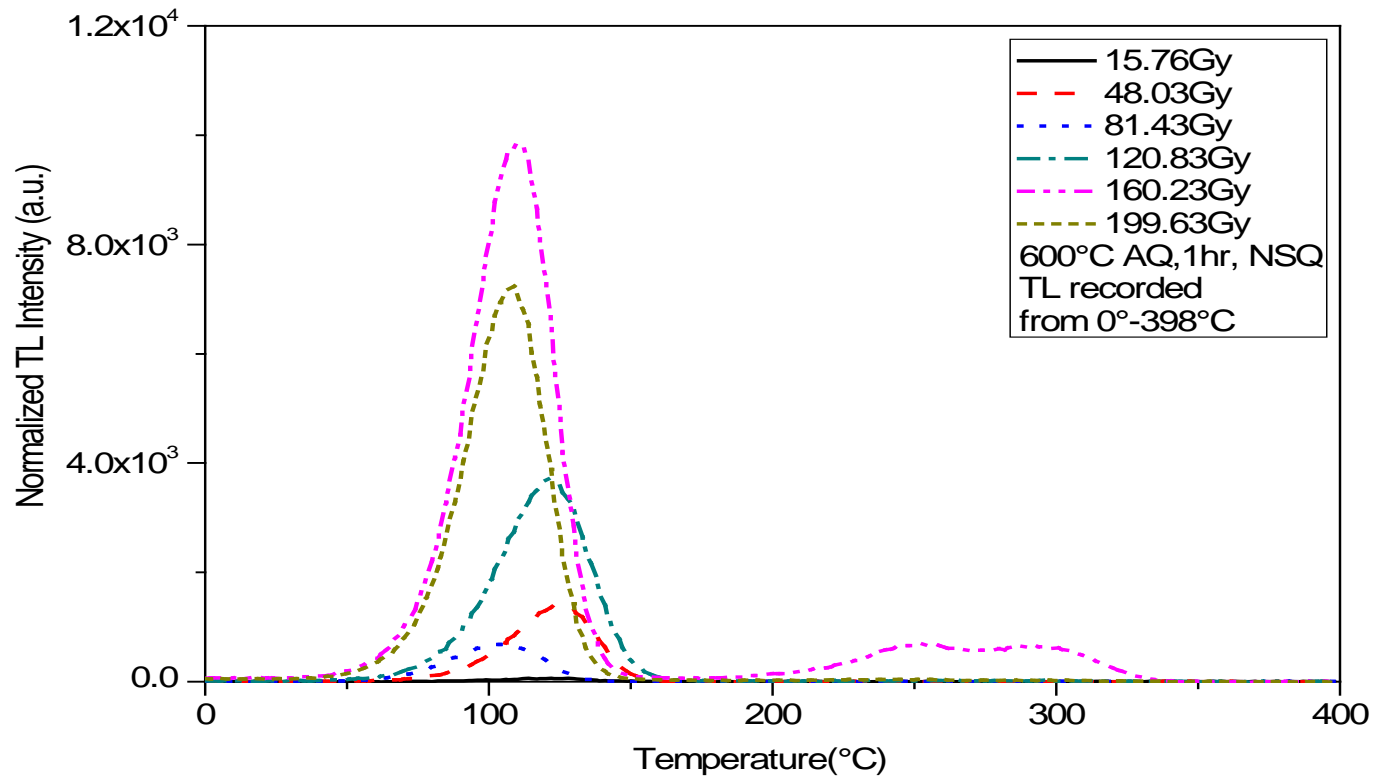


Fig. 5.2 TL glow curve of 400°C annealed NSQ for different beta doses.



**Fig. 5.3** TL glow curve of 600°C annealed NSQ for different beta doses.

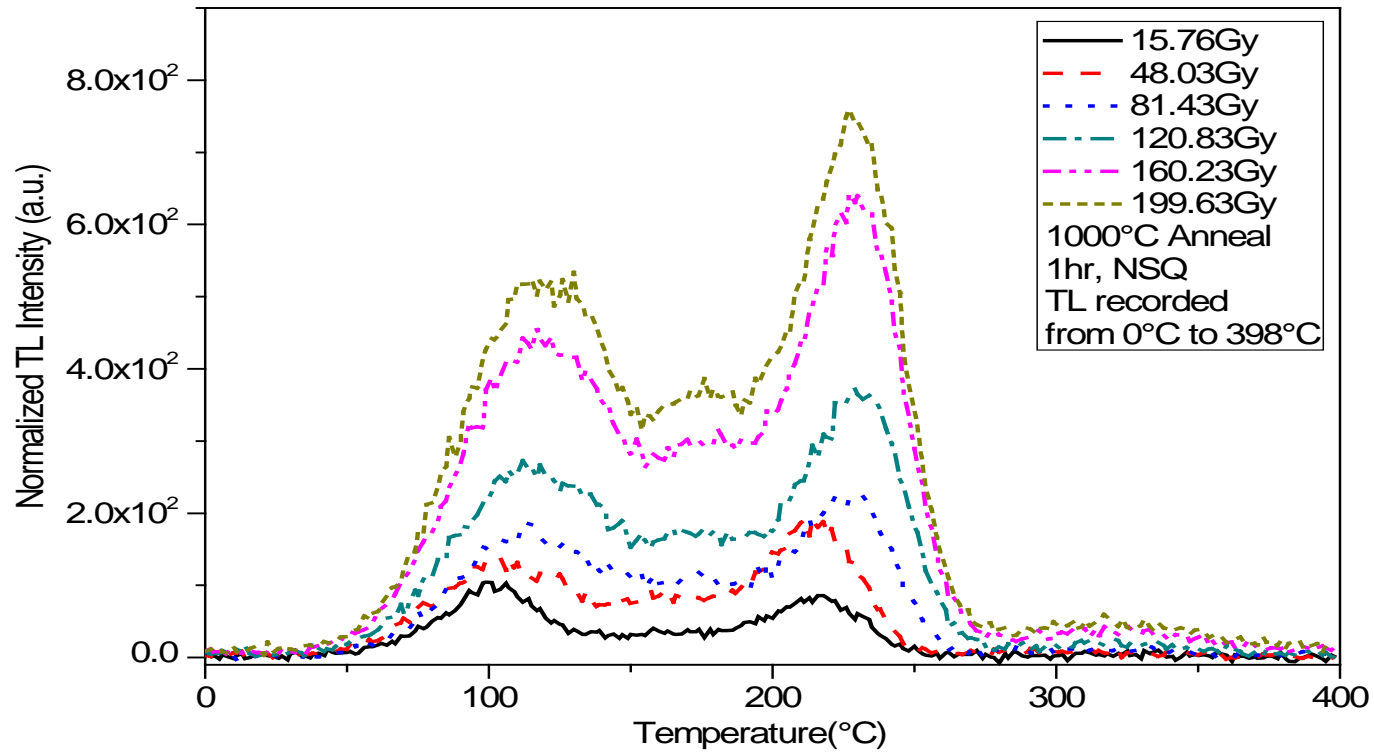
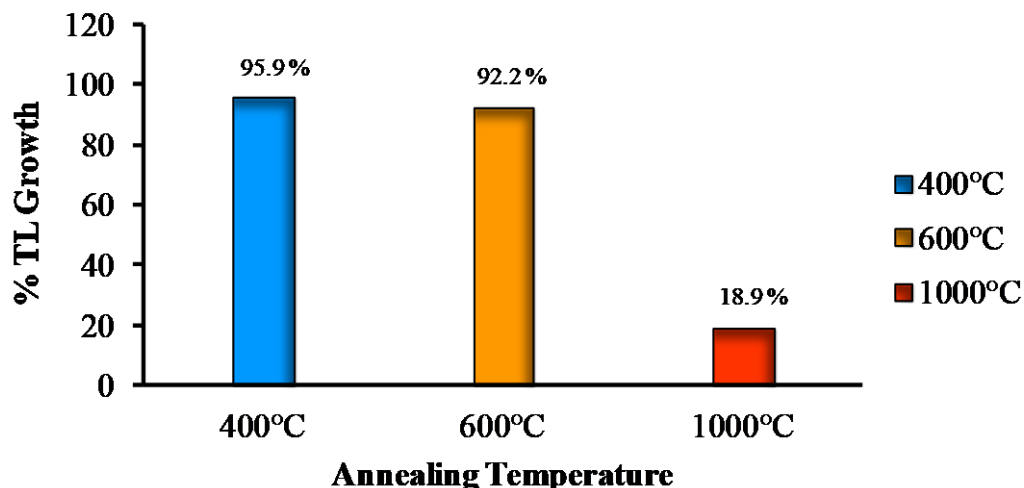


Fig. 5.4 TL glow curve of 1000°C annealed NSQ for different beta doses.

The significant contribution of 110°C TL glow peak was continued similarly as in earlier samples and intensity of this peak increased from 104 counts to 522.2 counts with respect to the beta doses for 1000°C thermally treated specimens. However, under this annealing treatment, the span of scattered TL glow peaks decreased and it approached towards the stability of TL glow peak at temperatures between 220°C-230°C. The growth of 220°C TL peak was observed from 86 counts to 759.6 counts with increase in beta doses along with humps around 158-176°C. It was noticed that the strength of TL counts of 110°C glow peak significantly reduced with rise in annealing temperature followed by identical beta radiations. In other words, the 400°C annealed NSQ sample showed significant TL strength of 110°C glow peak compared to 600°C and 1000°C annealed samples. It is also significant to observe that higher annealed NSQ samples (1000°C for 1hr) considerably reduced the span of TL glow peaks. This higher anneal temperature also helped to establish better thermal stability and systematic TL growth of 220°C glow peak. **(Fig. 5.4)**

### **5.2.3 Comparative TL study between unannealed and annealed NSQ samples for beta doses.**

The effects of annealing treatments on TL intensities of glow peaks of interest were compared with unannealed samples under identical beta exposures. The TL of 110°C glow peak for 400°C annealed samples grew up to 95.90% compared to unannealed samples. The average TL growth percentages of the same peak were observed 92.22% for 600°C annealed samples whereas 18.95% for 1000°C annealed samples as compared to unannealed samples **(Fig. 5.5)**. It is clearly suggested that the lower annealing treatments of 400°C to NSQ samples were more effective for the average TL growth of 110°C glow peak. However, the 1000°C annealing treatment followed by 160.23Gy and 199.23Gy doses supported to enhance the average TL growth percentages by 56.71% for 230°C TL glow peak **(Table 5.1)**.



**Fig. 5.5** Average TL growth percentages for 110°C glow peak of NSQ samples annealed at 400°C, 600°C and 1000°C w.r.t. unannealed NSQ sample.

**Table 5.1** Average TL growth percentages for 230°C glow peak of NSQ sample annealed at 1000°C w.r.t. unannealed NSQ sample.

Sr. No.	Dose	Unannealed		1000°C AQ		TL Growth % of 1000°C AQ w.r.t. Unannealed
		TL Peak	TL Counts	TL Peak	TL Counts	
1	160.23	214	195.2	230	640	69.50
2	199.63	219	426	227	759.6	43.92
Mean						56.71

Kale Y D have reported that annealing-quenching treatment to the crystalline material enhances thermal sensitization and shows phase transformation at definite temperature<sup>3</sup>. According to their work<sup>13</sup>, the  $\alpha$ -Quartz was stable below 573°C and showed Trigonal structure, the  $\beta$ -Quartz was stable from 573°C to 870°C and showed Hexagonal structure, whereas; both the  $\alpha$  and  $\beta$ -Tridymite phase showed Orthorhombic structure, exist metastable from 117°C to 163°C and were never stable. But, the  $\beta_2$ -Tridymite was stable from 867°C to 1470°C and exist metastable from 163°C to 867°C with Hexagonal structure. The TL sensitization of 110°C glow peak with followed annealing treatments for NSQ crystals, in present studies also is in agreement with first transformation from alpha to beta phase. This transformation seems to be responsible for enhancement of 110°C TL glow peak in 400°C annealed NSQ samples. ESR studies of such specimens also confirm that annealing temperature is responsible for increment of thermal sensitization of defects

level related to  $E_1'$  centres. However, it is also discernible that the reduction in TL strength by further annealing at higher temperature while sustaining 110°C glow peak position may be due to reduction in concentration of the  $E_1'$  centres in NSQ sample. In yet another significant development it was observed that under the influence of higher annealing treatment, the variation in TL glow peaks at higher temperature were decreased so as to obtain the better thermal stability in TL glow peak around 220°C. The loss in TL strength of 110°C glow peak in NSQ is attributed to reduced concentration of  $E_1'$  centres development but the new TL glow peak at 220°C may be ascribed to growth of Ge centres. This is also confirmed with ESR study of such annealed NSQ samples.

Toktamis et al. and McKeever et al. reported that changes in TL glow peak pattern under influence of optical bleaching have significance for the dating and dosimetric applications aspects<sup>14-16</sup>. They also explained that the traps which have been developed in the sample under influence of physical conditions/treatments may be optically or thermally sensitive in nature, hence, the bleaching by an optical source of definite wavelength has strength to release trapped electrons from definite trap depth and recombine to recombination centre. It enhances the luminescence output by releasing electron from particular trap and reduced the loss of charges by disconnected traps. Similarly, optical bleaching at chosen elevated temperature also has ability to erase shallow traps and transfer electrons from shallow traps to the stable TL traps which could be beneficial for dosimetric purpose<sup>3,17</sup>. With this view, TL glow curves of NSQ specimens were also recorded for identical physical treatments after Optical bleaching at 470nm at room temperature as well as at a chosen 160°C.

#### **5.2.4 Effect of optical bleaching temperatures on TL of unannealed and annealed NSQ specimens.**

The unannealed NSQ samples followed by beta 160.23Gy and 199.63Gy beta doses were bleached for 100seconds by definite wavelength (470nm blue light) at room temperature as well as at 160°C elevated temperature (ET). The changes in TL glow curve pattern were examined and found that the optical bleaching near room temperature, the unannealed samples gave major existence of 110°C, 165°C and 220°C TL glow peaks with growth under

influence of beta radiations (**Fig. 5.6**). The TL signal strength of 220°C TL glow peak was better than TL signal strength of 110°C and 165°C glow peaks. The stable peak around 220°C TL peak of quartz has been widely used for dose measurement and dating<sup>18</sup>. Kale Y D et al. suggested that the TL glow curves of synthetic quartz before and after OSL for 220°C TL glow peak was stable and sensitive under illumination of light<sup>19</sup>.

It may be indicated that during optical bleaching at room temperature for NSQ specimens, the charges were released from optically sensitive traps and majority of them were transferred toward the 220°C TL trap and showed stability at room temperature. Thus, it might be responsible for the growth of 220°C TL peak.

Further, to understand the behaviour of 220°C TL glow peak under the influence of optical bleaching, identical physically treated samples were optically bleached by chosen wavelength at 160°C for 100 seconds and the changes in TL glow curves pattern were recorded and studied. The NSQ sample exhibited single contribution of stable TL glow peak at 230°C with growth of this peak with rise in beta doses (**Fig. 5.7**). In presence of followed protocol, the charges might have been released from optically sensitive traps due to optical energy and it may transferred toward TL traps above 160°C due to restriction of optical bleaching temperature. In other words, bleaching at definite elevated temperature may avoid re-trapping of optically released charges into shallow traps. It may attribute to equivalent process of recuperation by optical bleaching and thermal erosion of shallow TL traps up to 160°C temperature (combine physical effect). These combine physical effect seems to be responsible for the development of another stable TL glow peak at 230°C, which might correspond to family of stable TL trap in NSQ sample.

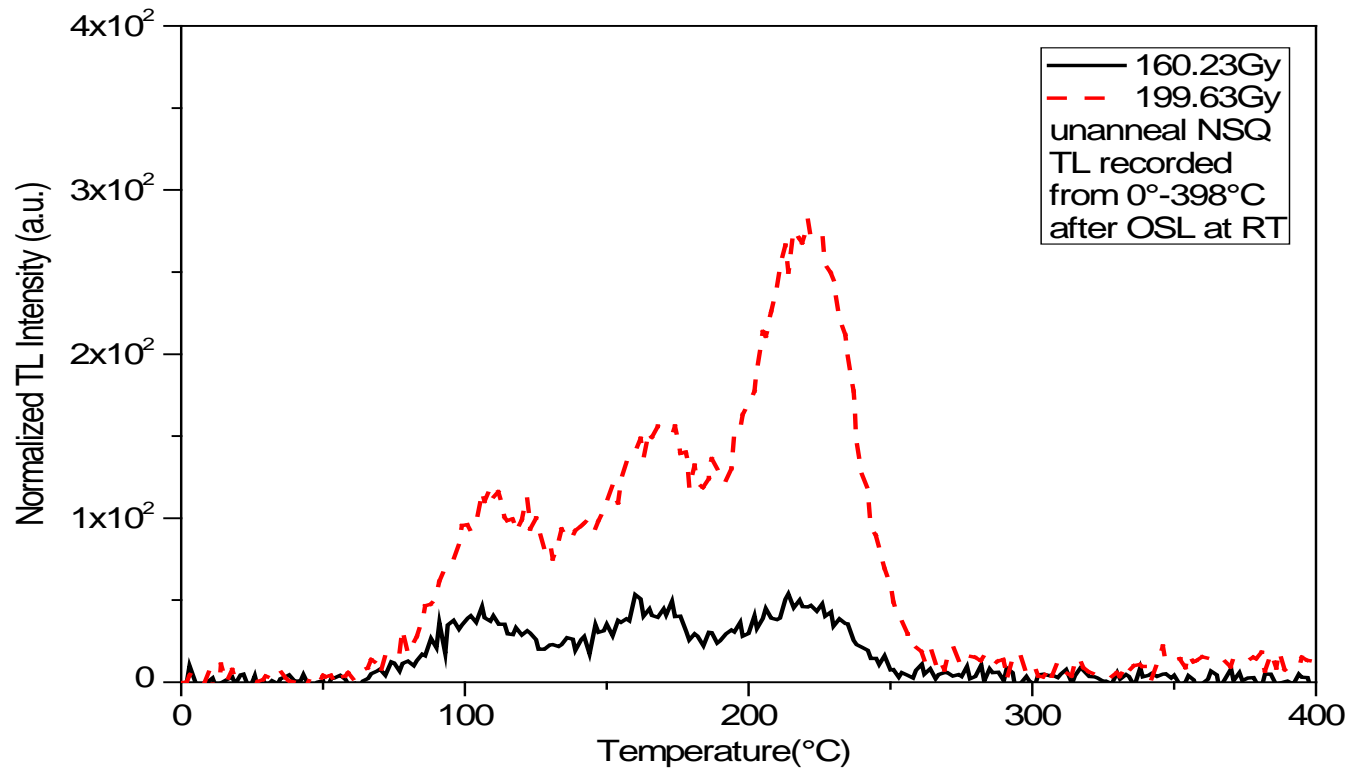


**Fig. 5.6** TL glow curve after OSL (at RT) of unannealed NSQ samples.

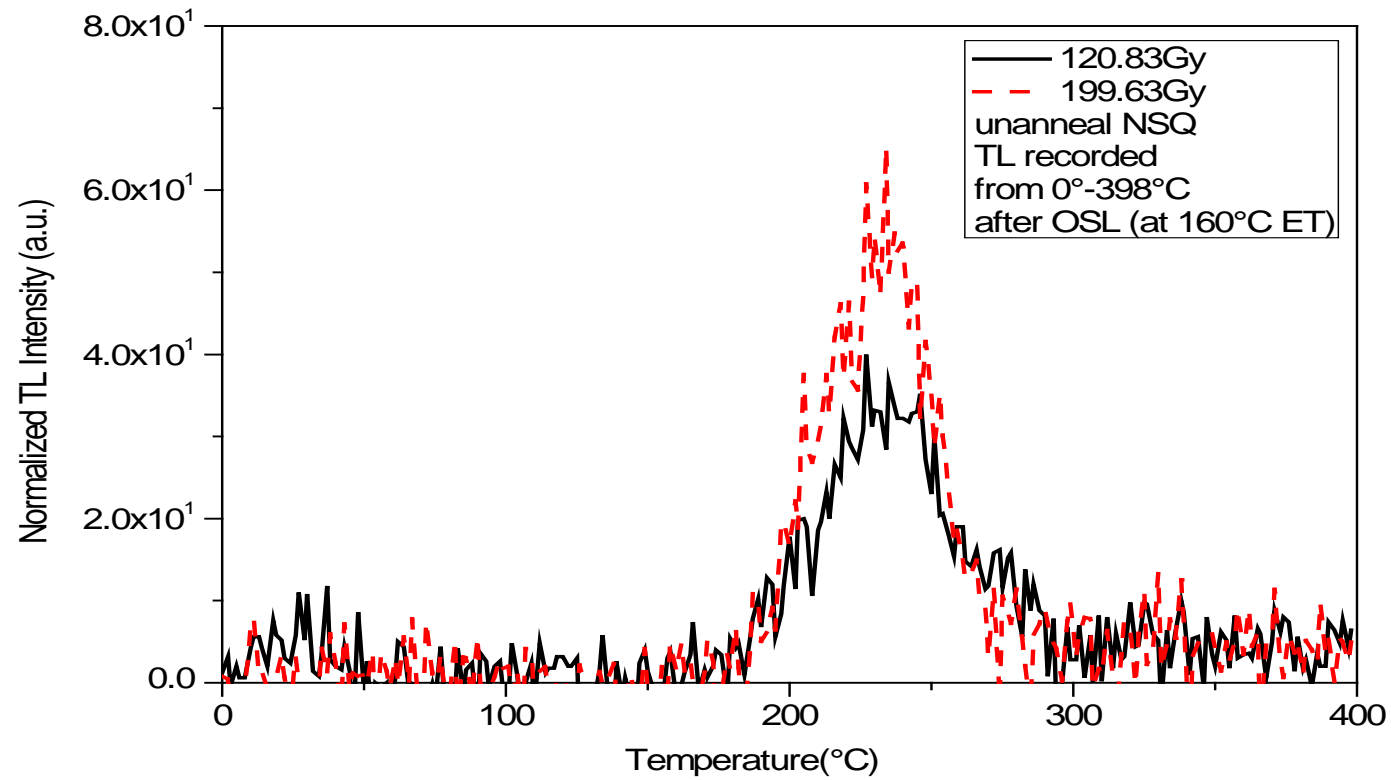
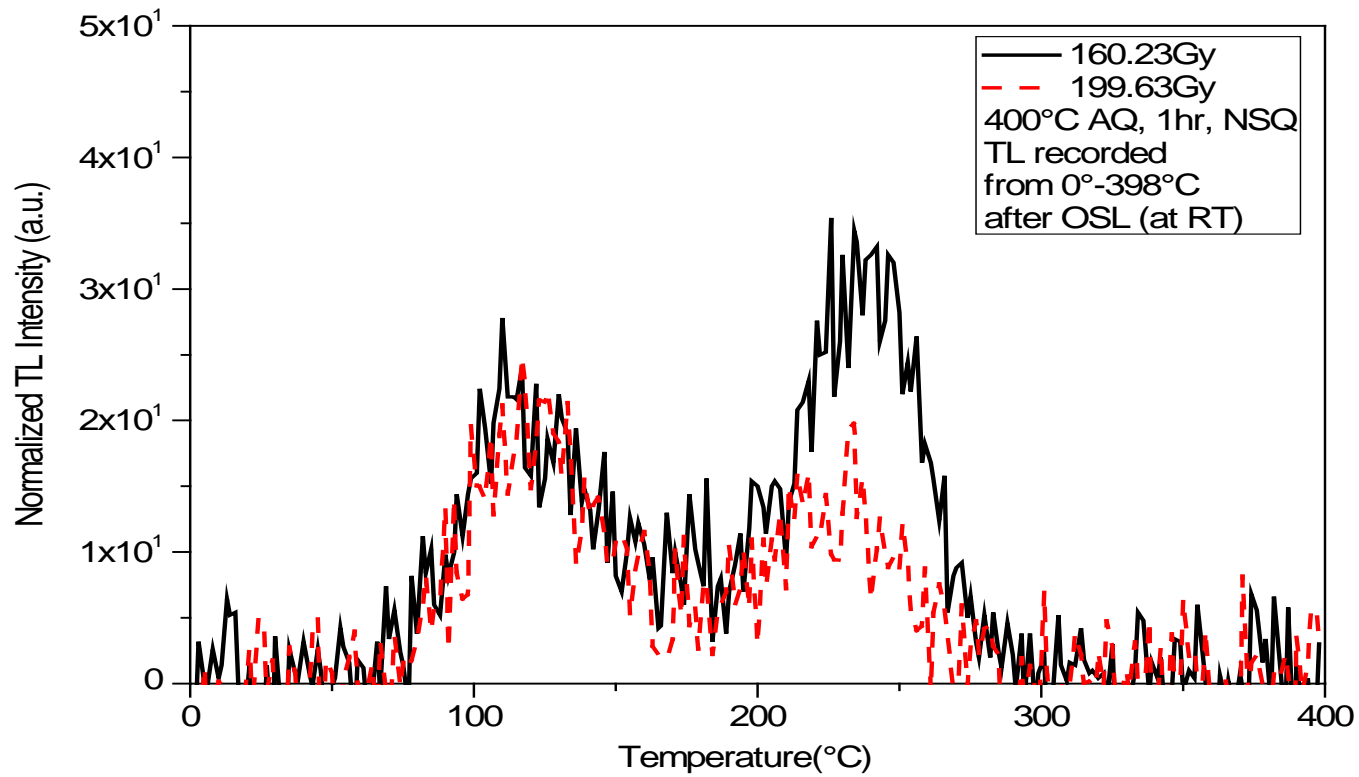
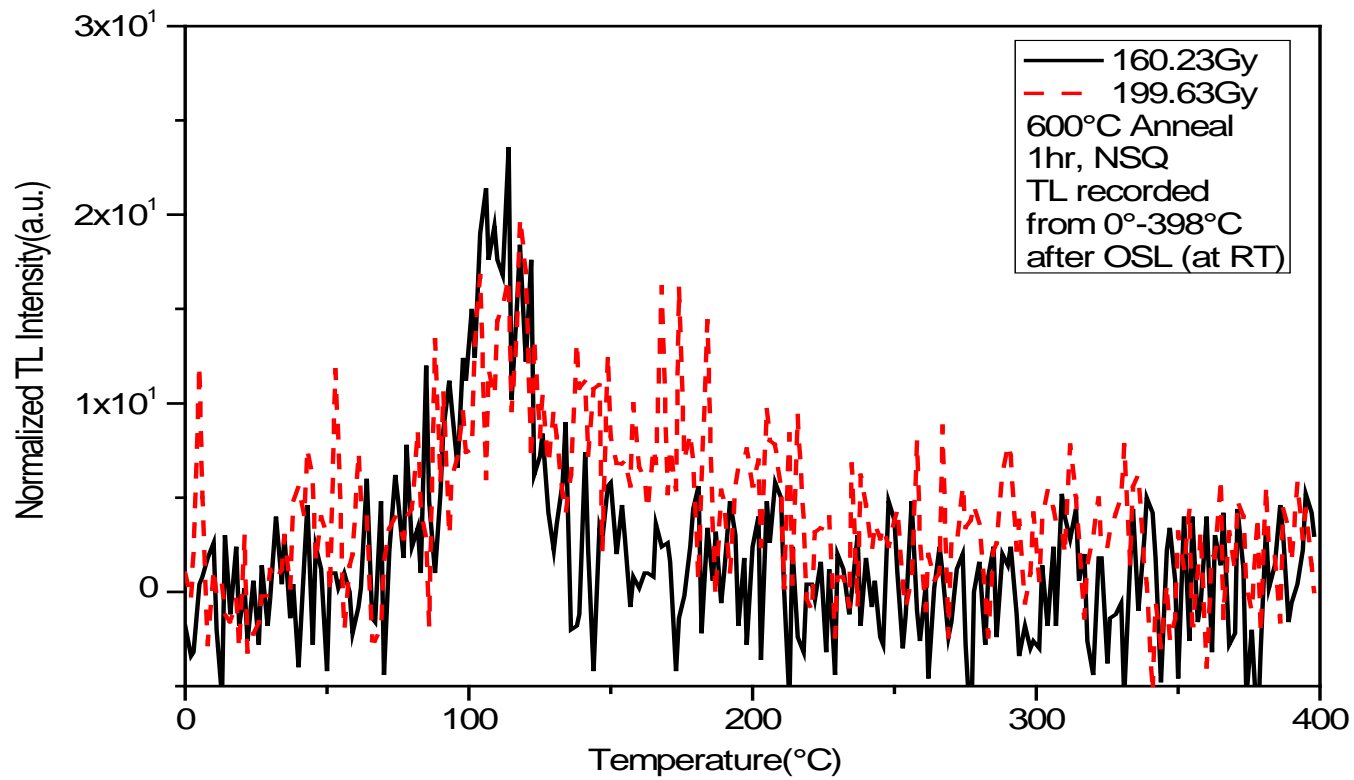


Fig. 5.7 TL glow curve after OSL (at 160°C ET) of unannealed NSQ samples.

With a view to understand the effect of optical bleaching temperatures on TL of annealed NSQ specimens were also considered. The lower annealed samples followed by 160.23Gy and 199.23Gy beta radiation doses were optically bleached near room temperature showed typical contribution of 110°C TL glow peak with little bit development of 230°C TL glow peak (**Fig. 5.8 & Fig. 5.9**). Whereas the NSQ sample annealed at 1000°C of 1 hour duration followed by identical beta radiation doses, were optically bleached at room temperature showed typical contribution of 110°C TL glow peak along with the clear exhibition of 220°C TL glow peak along with a new 300°C TL glow peak. Also, the close examination of TL sensitivities of these glow curves revealed that the TL glow peak sensitivity increases with rise in beta doses up to 120.83Gy and reduced by further rise in beta doses (**Fig. 5.10**).



**Fig. 5.8** TL glow curve after OSL (at RT) of 400°C annealed NSQ samples.



**Fig. 5.9** TL glow curve after OSL (at RT) of 600°C annealed NSQ samples.

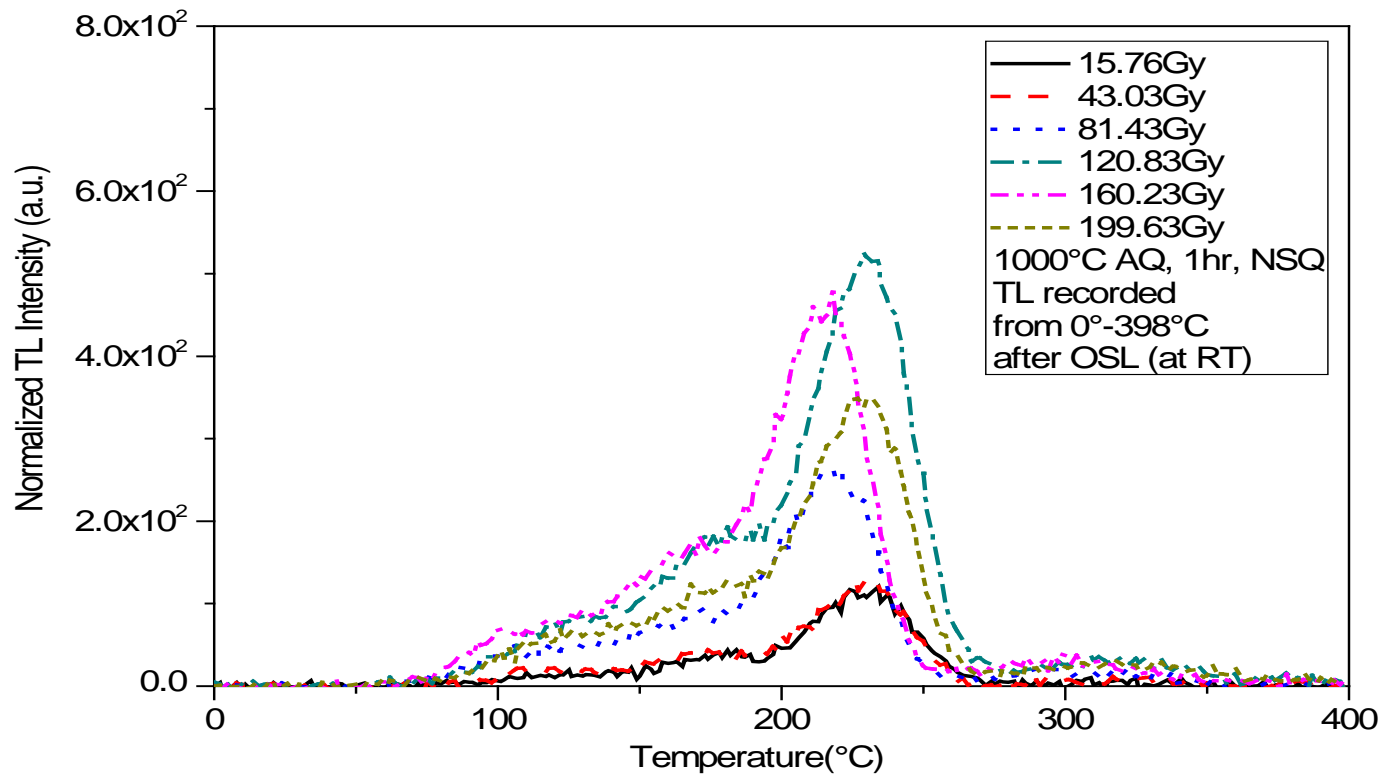


**Fig. 5.10** TL glow curve after OSL (at RT) of 1000°C annealed NSQ samples.

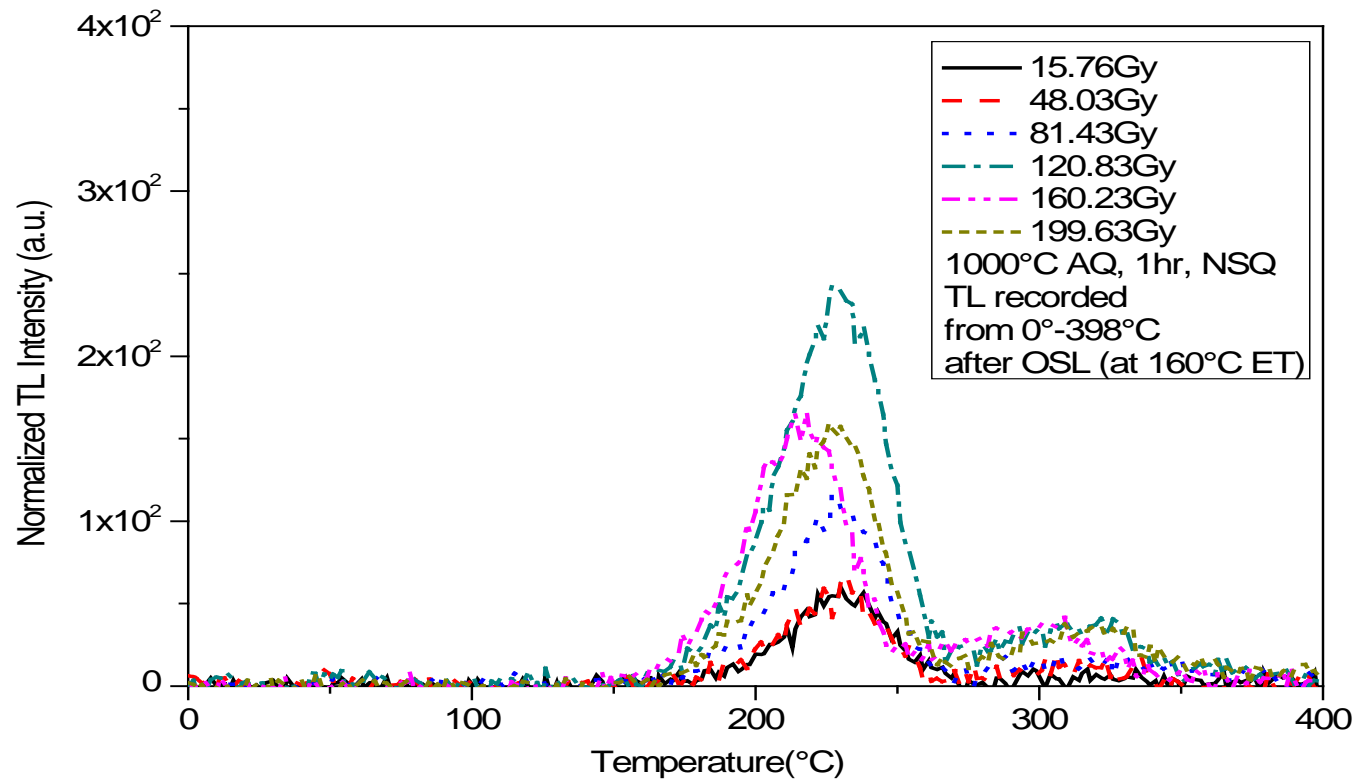


**Fig. 5.11** TL glow curve after OSL (at 160°C ET) of 1000°C annealed NSQ samples.

To understand further, the studies were concentrated for NSQ specimens annealed at 1000°C only due to the interest in stable peak around 220°C TL glow peak. The NSQ sample annealed at 1000°C followed by identical beta doses were optically bleached at 160°C for 100seconds. Under the influence of optical bleaching at the chosen elevated temperature, the contribution of shallow 110°C TL glow peak disappeared clearly. The well-established thermally stable TL glow peak was exhibited at 230°C along with new development of TL glow peak at 325°C for these experimental conditions. The TL growth patterns of 230°C glow peaks with optical bleaching at elevated temperature are similar to that of the TL growth pattern of peaks under optical bleaching at room temperature (**Fig. 5.11**).

Mckeever et al. and Botter-Jensen et al. have reported that optical bleaching by suitable wavelength offered optical erosions of the charges from suitable light sensitive traps. There are few possibilities either optically released charges may re-trapped into same traps or re-trapped into other localities or recombine with recombination centres. According to the luminescence model, during optical bleaching, the optically sensitive traps participate and support for desired TL<sup>17,20</sup>. The TL results of NSQ specimens with optical bleaching at room temperature also revealed re-trapping of optically released charges. While, the development of 230°C TL glow peaks under influence of optical bleaching at 160°C reveals clearly the thermally stable TL glow peaks range within 220°C-230°C along with rapidly bleachable TL glow peaks within 300°C-325°C.

### **5.2.5 Comparative TL study between unannealed and annealed NSQ samples followed by beta doses and optical bleaching temperatures.**

The average TL growth percentages of glow peaks were reduced significantly under the influence of optical bleaching at room temperature (**Table 5.2**), (**Table 5.3**), (**Table 5.4**). However, the optical bleaching at 160°C eliminated the contribution of 110°C and 165°C glow peaks and offered the shifting of TL glow peak from 220°C to 230°C (**Table 5.5**). But, the optical bleaching at elevated temperature was found more effective to bleach average TL counts over optical bleaching at room temperature (**Table 5.6**).

**Table 5.2** Average TL growth percentages for 110°C glow peak of unannealed NSQ with optical bleaching w.r.t. unannealed NSQ without optical bleaching at RT.

Sr. No.	Dose (Gy)	TL Peak (°C)	TL counts for Unannealed without bleaching	TL counts for Unannealed with bleaching at RT	TL Growth % of Unannealed with bleaching w.r.t. Unannealed without bleaching
1	160.23	110	553.2	40.6	-1262.56
2	199.63	110	617.6	118.8	-419.87
<b>Mean</b>					<b>-841.21</b>

**Table 5.3** Average TL growth percentages for 165°C glow peak of unannealed sample with optical bleaching w.r.t. unannealed sample without optical bleaching at RT.

Sr. No.	Dose (Gy)	TL Peak (°C)	TL counts for Unannealed without bleaching	TL counts for Unannealed with bleaching at RT	TL Growth % of Unannealed with bleaching w.r.t. Unannealed without bleaching
1	160.23	165	179.8	44.8	-301.34
2	199.63	171	332.8	156	-113.33
<b>Mean</b>					<b>-207.34</b>

**Table 5.4** Average TL growth percentages for 220°C glow peak of unannealed sample with optical bleaching w.r.t. unannealed sample without optical bleaching at RT.

Sr. No.	Dose	Unannealed without bleaching		Unannealed with bleaching at RT		TL Growth % of Unannealed with bleaching w.r.t. Unannealed without bleaching
		TL Peak	TL counts	TL Peak	TL counts	
1	160.23	214	195.2	218	50.20	-288.84
2	199.63	219	426	221	218.80	-94.70
<b>Mean</b>						<b>-191.77</b>

**Table 5.5** Average TL growth percentage for 220°C glow peak of unannealed sample with optical bleaching w.r.t. unannealed sample without optical bleaching at 160°C.

Sr. No.	Dose	Unannealed without bleaching		Unannealed with bleaching at 160°C		TL Growth % of Unannealed with bleaching at 160°C w.r.t. Unannealed without bleaching
		TL Peak	TL counts	TL Peak	TL counts	
1	160.23	214	195.2	232	47.80	-308.37
2	199.63	219	426	234	65.20	-553.37
<b>Mean</b>						<b>-430.87</b>

**Table 5.6** Average TL growth percentages for 230°C glow peak of unannealed sample with optical bleaching at 160°C w.r.t. unannealed sample with optical bleaching at RT.

Sr. No.	Dose	Unannealed with bleaching at RT		Unannealed with bleaching at 160°C		TL Growth % of Unannealed with bleaching at 160°C w.r.t. Unannealed with bleaching at RT
		TL Peak	TL counts	TL Peak	TL counts	
1	160.23	<b>218</b>	50.2	<b>232</b>	47.80	-5.02
2	199.63	<b>221</b>	281.8	<b>234</b>	65.20	-332.21
<b>Mean</b>						<b>-173.29</b>

Further, the TL outcomes were compared between 1000°C annealed samples followed by beta doses and optically bleached at room temperature. The optical bleaching at room temperature showed the existence of 110°C and 220°C TL glow peaks. Also, it revealed that the development of 300°C TL peaks. The average TL counts percentage of 110°C TL glow peak decreases rapidly whereas average TL counts percentage of 220°C TL glow peak decreases slowly with optical bleaching of NSQ at Room temperature. It clearly means that the 1000°C annealed samples shows slower bleaching of 220°C TL glow peak.

Further in a yet significant observation, it was found that 300°C TL glow peak which was present in unannealed NSQ samples followed by beta doses below 120.83Gy and was absent in 1000°C annealed with identical beta doses, reappears after optical bleaching at room temperature. It is suggested to be the subsidiary contribution of the family of typical rapidly bleachable TL glow peaks. It is reasonable to believe that its closeness with typical rapidly bleachable TL glow peak, charges must have been transferred to reappear as an unusual rapidly bleachable TL glow peak during bleaching process. (**Table 5.7, Table 5.8**).

**Table 5.7** Average TL growth percentages for 110°C glow peak of 1000°C AQ sample with optical bleaching w.r.t. 1000°C AQ sample without optical bleaching at RT.

Sr. No.	Dose	TL Peak	TL counts for 1000°C AQ without bleaching	TL counts for 1000°C AQ with bleaching at RT	TL Growth % of 1000°C AQ with bleaching w.r.t. 1000°C AQ without bleaching
1	15.76	101	104	13.6	-664.71
2	48.03	104	138.4	22.4	-517.86
3	81.43	112	185.8	53.6	-246.64
4	120.83	112	273.4	77.6	-252.32
5	160.23	117	454.8	78.8	-477.16
6	199.63	118	522.2	68.2	-665.69
<b>Mean</b>					<b>-470.73</b>

**Table 5.8** Average TL growth percentages for 220°C glow peak of 1000°C AQ sample with optical bleaching w.r.t. 1000°C AQ sample without optical bleaching at RT.

Sr. No.	Dose	TL Peak	TL counts for 1000°C AQ without bleaching	TL counts for 1000°C AQ with bleaching at RT	TL Growth % of 1000°C AQ with bleaching w.r.t. 1000°C AQ without bleaching
1	15.76	218	86	120.4	28.57
2	48.03	214	193.8	133	-45.71
3	81.43	222	222.6	264.2	15.75
4	120.83	229	371.8	524.6	29.13
5	160.23	230	640	478	-33.89
6	199.63	227	759.6	349.4	-117.40
<b>Mean</b>					<b>-20.59</b>

The bleaching at 160°C shifts the stable 220°C TL glow peak to the stable TL glow peak at 230°C by transferring of charges under influence of combine recuperation process (optical bleaching and thermal erosion from shallow traps). The average TL counts percentage of 230°C TL glow peak comparatively reduces faster with optical bleaching at 160°C than average TL counts percentage without optical bleaching. **(Table 5.9)**

The bleaching at 160°C is suggestive of the thermal stability of 230°C TL glow peak. It also demonstrates subsidiary contribution of usual rapidly TL glow peak. The optical bleaching at 160°C was more effective to remove average TL growth percentage from material than the optical bleaching at room temperature **(Table 5.10)**.

**Table 5.9** Average TL growth percentages for 230°C glow peak of 1000°C AQ sample with optical bleaching in w.r.t. 1000°C AQ sample without optical bleaching at 160°C.

Sr. No.	Dose	1000°C AQ without bleaching		1000°C AQ with bleaching at 160°C		TL Growth % of 1000°C AQ with bleaching at 160°C w.r.t. 1000°C AQ without bleaching
		TL Peak	TL counts	TL Peak	TL counts	
1	15.76	<b>218</b>	86	<b>230</b>	60.2	-42.86
2	48.03	<b>214</b>	193.8	<b>232</b>	67.8	-185.84
3	81.43	<b>222</b>	222.6	<b>227</b>	117	-90.26
4	120.83	<b>229</b>	371.8	<b>218</b>	242.6	-53.26
5	160.23	<b>230</b>	640	<b>230</b>	166	-285.54
6	199.63	<b>227</b>	759.6	<b>227</b>	157.6	-381.98
<b>Mean</b>						<b>-173.29</b>

**Table 5.10** Average TL growth percentages for 230°C glow peak of 1000°C AQ sample with optical bleaching at RT in w.r.t. 1000°C AQ sample with optical bleaching at 160°C.

Sr. No.	Dose	1000°C AQ with bleaching at RT		1000°C AQ with bleaching at 160°C		TL Growth % of 1000°C AQ with bleaching at RT w.r.t. 1000°C AQ with bleaching at 160°C
		TL Peak	TL counts	TL Peak	TL counts	
1	15.76	<b>234</b>	120.4	<b>230</b>	60.2	-100.00
2	48.03	<b>232</b>	133	<b>232</b>	67.8	-96.17
3	81.43	<b>218</b>	264.2	<b>227</b>	117	-125.81
4	120.83	<b>229</b>	524.6	<b>227</b>	242.6	-116.24
5	160.23	<b>218</b>	478	<b>218</b>	166	-187.95
6	199.63	<b>227</b>	349.4	<b>230</b>	157.6	-121.70
<b>Mean</b>						<b>-124.65</b>

### 5.2.6 TL-Dose Response Curve (DRC) study of NSQ samples.

The characteristics of TL-DRC represented by the magnitude of slope of the graph over log (TL-Intensity)-log (Dose) scale<sup>21</sup>. The magnitude of slope can be calculated by the relation between TL and Dose,

$$TL\ Intensity = aD^k$$

Where,  $a$  is constant,  $D$  is applied dose,  $k$  value is related to slope of the DRC and it represent that graph is super-linear if  $k > 1$ ; linear if  $k = 1$  and sub-linear if  $k < 1$ .

### 5.2.6.1 TL-DRC study of unannealed NSQ samples.

The unannealed samples showed predominant contribution of 110°C TL glow peak with uniform TL growth under influence of 48.03Gy, 81.43Gy, 120.83Gy, 160.23Gy and 199.63Gy beta doses. The  $k$  value was calculated for TL dose response curve of 110°C glow peak and found to be 1.57 which suggested super-linear TL-DRC characteristics of 110°C TL glow peak of NSQ material (**Table 5.11**).

**Table 5.11** Observation for TL-DRC of Unannealed, 400°C, 600°C and 1000°C annealed NSQ samples.

Sr. No.	Sample description	TL Glow Peak	Slope (k)	Nature of Dose Response Curve
1	Un-annealed	at 110°C	1.57	Supra-linear
2	400°C Annealed	at 110°C	1.19	Supra-linear
3	600°C Annealed	at 110°C	1.91	Supra-linear
4	1000°C Annealed	at 110°C	0.65	Sub-linear
5		at 175°C	0.86	Sub-linear
6		at 220°C	0.85	Sub-linear
7		at 110°C after OSL at RT	0.75	Sub-linear
9		at 220°C after OSL at RT	0.59	Sub-linear
10		at 220°C after OSL at 160°C	0.49	Sub-linear

The nature of dose dependence of TL signals is important for its use for dosimetry, geological and archaeological dating<sup>22</sup>. Chen R et al. have reported that 110°C TL glow peak of unannealed synthetic quartz showed strong super-linear behaviour with doses<sup>23</sup>. Scientists suggested two model for super-linearity, in which one involve competition mechanism during excitation (absorption stage), and second one involve competition mechanism during heating (recombination stage)<sup>24</sup>. Prepared unannealed NSQ samples were also shows super-linear ( $k = 1.57$ ) characteristics of 110°C TL-DRC. It means that competition mechanism was involved in TL output signals of unannealed NSQ.

### 5.2.6.2 TL-DRC study of annealed NSQ samples.

The TL-DRC was recorded for annealed NSQ samples as well and hence  $k$  value was also calculated for TL-DRC of observed glow peaks. The 400°C and 600°C annealed specimens showed major contribution of 110°C TL glow peak with uniform TL growth. These annealed samples showed  $k$  value of TL-DRC

curve about 1.19 and 1.91 for 400°C and 600°C annealed specimens respectively for this peak. The size of  $k$  value suggested super-linear TL-DRC nature of 110°C TL glow peak of annealed NSQ samples.

The significant changes in strength of TL-DRC were observed in 1000°C annealed samples. It exhibited two more TL glow peaks at 165°C and 220°C accordance with 110°C TL glow peak. The suggested TL glow peaks showed weaker strength in TL growth with doses. The values of  $k$  were 0.65, 0.86 and 0.85 for 110°C TL glow peak, for 165°C TL glow peak and for 220°C TL glow peak respectively. The 1000°C annealed samples exhibit sub-linear characteristics of TL dose response curve to TL glow peaks of interest (**Table 5.11**).

Chen et. al worked on synthetic quartz and they concluded that TL dose response behaviour is extremely dependent on the firing temperature<sup>23</sup>. Charitidis et al. found that firing temperature removes competitors and resultant sensitivity is increased due to absence of competitors and superlinearity removed<sup>25</sup>. They related it with removal of competitors with phase transformation of quartz. In present work, superlinearity was observed for 110°C TL peak dose response at lower annealed NSQ samples (400°C and 600°C) and superlinearity was changed into sublinear for the same TL peak as annealing temperature for NSQ raised to 1000°C temperature. On the other side, TL-DRC nature of 165°C and 220°C TL glow peaks was also showing sub-linear dose response. Hence, it is reasonable to believe that competitors were removed at higher anneal temperature of NSQ sample with decrease in sensitivity.

### **5.2.6.3 TL-DRC study of annealed NSQ samples followed by optical bleaching temperatures.**

Under the influence of optical bleaching at room temperature, the 1000°C annealed NSQ samples TL-DRC of 110°C and 220°C TL glow peaks were plotted. The  $k$  value of both TL-DRC curves was less than 1.0 and hence it suggested sub-linear TL-DRC characteristics of chosen TL glow peaks (**Table 5.11**).

Under the influence of optical bleaching at an elevated temperature at 160°C, the 1000°C annealed NSQ samples exhibited existence of 230°C TL glow peak and hence it produced sub-linear characteristics of TL-DRC (**Table 5.11**).

Luminescence scientists suggested that all optically sensitive TL traps are involved in TL process but all thermally sensitive traps are not contributed in OSL process<sup>1</sup>. Considering this fact, present investigations is throwing light on behaviour of the TL traps after optical stimulation at RT and 160°C ET. Sublinear TL–DRC nature of 1000°C annealed NSQ sample was remaining same even after optical bleaching at RT as well as ET. Thus, it can be concluded that competitors may not participate in TL output signals before or after optical bleaching. That means optical bleaching at RT or ET has no roll with trap competitors in any TL process.

The 1000°C annealed samples changed the super-linear to sub-linear TL-DRC nature of 110°C TL glow peak. It gave additional development of 165°C and 220°C glow peaks with sub-linear nature of TL-DRC. The optical beaching at 160°C temperature sustained sub-linear nature of TL-DRC curve for 220°C and 230°C TL glow peaks (**Table 5.11**).

### **5.3 OSL study of NSQ samples at room temperature**

OSL technique is well established tool for dose estimation of various phosphors and age determination of geological /archaeological samples. Literature claims the OSL technique is beneficial over the TL technique<sup>1,20</sup>. Silva E C et al. and Bhatt B C had studied OSL dose response, sensitivity, fading and dose reproducibility properties of nano phosphors and they have concluded that nano phosphor is good candidate for dosimetric applications and geological dating also<sup>26,27</sup>. The uses of either bulk or nano materials in OSL applications are explained by various suggested luminescence models and its mathematical simulation by assumption of luminescence parameters. The suggested luminescence models demonstrated that the treated phosphors contain thermally sensitive and optically sensitive traps. It is also reported that all OSL traps are responsible for TL process/outcome but all TL traps are not responsible for OSL process/outcome<sup>20</sup>. In other words, it may suggest that only few TL traps are having dual (thermal and optical) nature and hence it attribute to establish the correlation between TL and OSL. The pattern of OSL

decay curves reflects the recombination tendency of electron from trap into hole at recombination center. It is resolved by fast, medium and slow components of the OSL decay curve<sup>20</sup>. In this regard, the present work is aimed to give detailed insight about the interest in OSL properties of NSQ. Therefore, the OSL decay curves were recorded at room temperature for 100 seconds of optical stimulation with 470 nm. The resultant outcomes of OSL like structure of OSL decay curve, contribution of OSL components decay curve with their photo ionization cross-section, OSL intensity were studied under effect of (i) beta dose(s) (ii) annealing temperature(s) (iii) optical stimulation temperature at RT and ET. The comparisons are also being made between OSL outcomes for considered protocols then it was further understood by the OSL deconvolution results. The OSL deconvolution results included the information of OSL components and their photoionization cross-section. Moreover, the OSL dose response curves (DRC) were plotted and their characteristics were compared under identical conditions for further clarity.

### **5.3.1 Effect of beta doses on OSL decay recorded at room temperature (RT) for unannealed NSQ samples.**

The batches of unannealed NSQ samples were exposed for different beta doses such as 15.76Gy, 48.03Gy, 81.43Gy, 120.83Gy, 160.23Gy and 199.63Gy. The OSL decay curves were recorded at room temperature (25°C) for 100seconds by optical stimulation with 470nm light. Under the influence of beta doses, the OSL counts rapidly decrease within 0 to 0.4seconds of stimulation time however, during 0.4seconds to 100seconds of stimulation OSL counts decrease at a much slower rate. It was also observed that, as beta doses to the NSQ specimens increase up to 120.83Gy of radiations, the magnitudes of initial maxima of OSL counts also increases from 4570.2 counts to 42177.8 counts. But, the noticeable variation in OSL counts was observed by further rise in beta doses above 120.83Gy of radiations (**Fig. 5.12**).

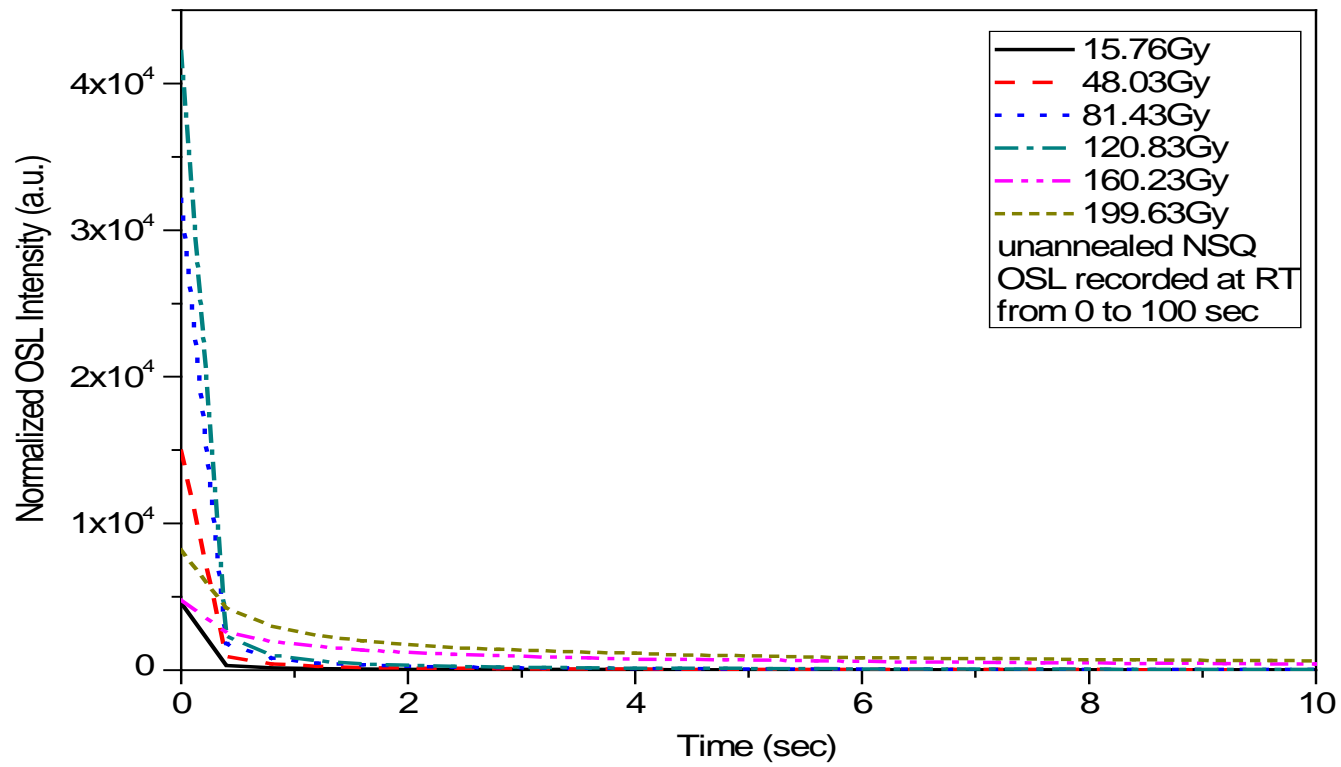


**Fig. 5.12** OSL Decay curve of unannealed NSQ at RT for different beta doses.

Botter-Jensen L and Kale Y D et al. have reported that under the influence of optical stimulation with selection of suitable visible light wavelength, the trapped electrons get ionized at definite energy levels. However, these electrons are released from corresponding optically sensitive traps and recombine with the hole at recombination centres via conduction band, this usual path of released electron offer standard OSL process. The graphical representation of typical OSL process follows the law of exponential decay which gives exponential shape of decay over the OSL intensity against stimulation time plot<sup>1</sup>. It is also reported that usual OSL process is influenced by physical treatments to the samples like ionising radiations, annealing treatment, stimulation wavelength, gains sizes and optical stimulation temperature<sup>1,28</sup>. Therefore, the common path of optically released electrons to recombination centre is changed and electron hole recombination happens with different path which gives the change in usual shape of OSL decay. The changes in usual path due to unusual OSL process offers various shapes of OSL decay curve under the influence of physical condition which gives unusual nature of OSL decay. Such unusual nature of OSL decay curves have two types of decay curves (i) initially, the  $I_{\max}$  OSL counts increases with stimulation time for few seconds thereafter  $I_{\max}$  OSL counts decreases with usual OSL decay for long time<sup>29</sup> (ii) the  $I_{\max}$  OSL counts drops very rapidly within few seconds of stimulation time thereafter OSL counts decrease as an usual OSL decay<sup>30</sup>. Owing to these complex observations, several OSL models have been developed and proposed to resolve them by deconvolution of OSL decay. McKeever SWS, reported that non-exponential patterns of OSL decay are responsible to predominant contribution of availability of shallow traps and re-trapping probability of optically released electrons either into suggested traps or into different localities<sup>17</sup>.

Frank et al have explained that during the initial part of the stimulation, OSL of natural quartz decays very rapidly and has been named as ultra-fast components (UFC)<sup>30</sup>. This component revealed availability of thermally unstable traps and thus can be removed by increasing pre-heat temperature prior to OSL measurements. The unannealed NSQ samples showed rapid OSL

decay within 0 to 0.4 seconds and usual OSL decay within 0.4 to 100 seconds of optical stimulation near room temperature.

Under the influence of various beta doses, the unannealed NSQ samples exhibited the rapid OSL decay within 0 to 0.4 seconds of stimulations and usual OSL decay within 0.4 to 100seconds of stimulation. The nature of rapid OSL decay was responsible is ascribed to the existence of UFC which were associated with available shallow optically sensitive unstable traps, whereas the nature of usual OSL decay was ascribed to predominant contribution of optically sensitive traps.

The growth of  $I_{\max}$  OSL counts depend upon dose of ionizing radiations. The variations in OSL counts with beta doses seem to be either due to saturation of OSL traps or growth of new OSL traps.

### **5.3.2 Effect of beta dose on OSL of annealed NSQ samples.**

In this part of the studies it is interesting to understand the behaviour of UFC, usual components of OSL decay and the OSL intensity of NSQ under effect of annealing treatments followed by identical doses. In view of this, the samples were annealed at 400°C, 600°C and 1000°C for one hour and quenched at room temperature then each batch of annealed-quenched sample was exposed to 15.76Gy, 48.03Gy, 81.43Gy, 120.83Gy, and 160.23Gy and 199.63Gy beta doses. The OSL decay curves of all such physically treated NSQ samples were recorded at room temperature.

Like unannealed NSQ samples, the annealed samples exhibited rapid OSL decay within 0 to 0.4 seconds and usual OSL decay within 0.4 to 100 seconds of stimulations. It is reasonable to suggest that contribution of proposed UFC and usual components still exist. The 400°C annealed NSQ sample displayed identical OSL growth pattern (from 117210.4 counts to 623454.8) as observed in OSL pattern of unannealed sample (**Fig. 5.13**). However, the 600°C and 1000°C annealed samples showed uniform OSL growth from 29267.4 counts to 172102.2 counts and from 1713.4 counts to 10157.6 counts up to 160.23Gy of doses respectively and thereafter it showed variation in OSL counts by further rise in beta doses. But, higher annealed samples offered weaker OSL strength under influence of identical beta doses (**Fig. 5.14 and Fig. 5.15**).

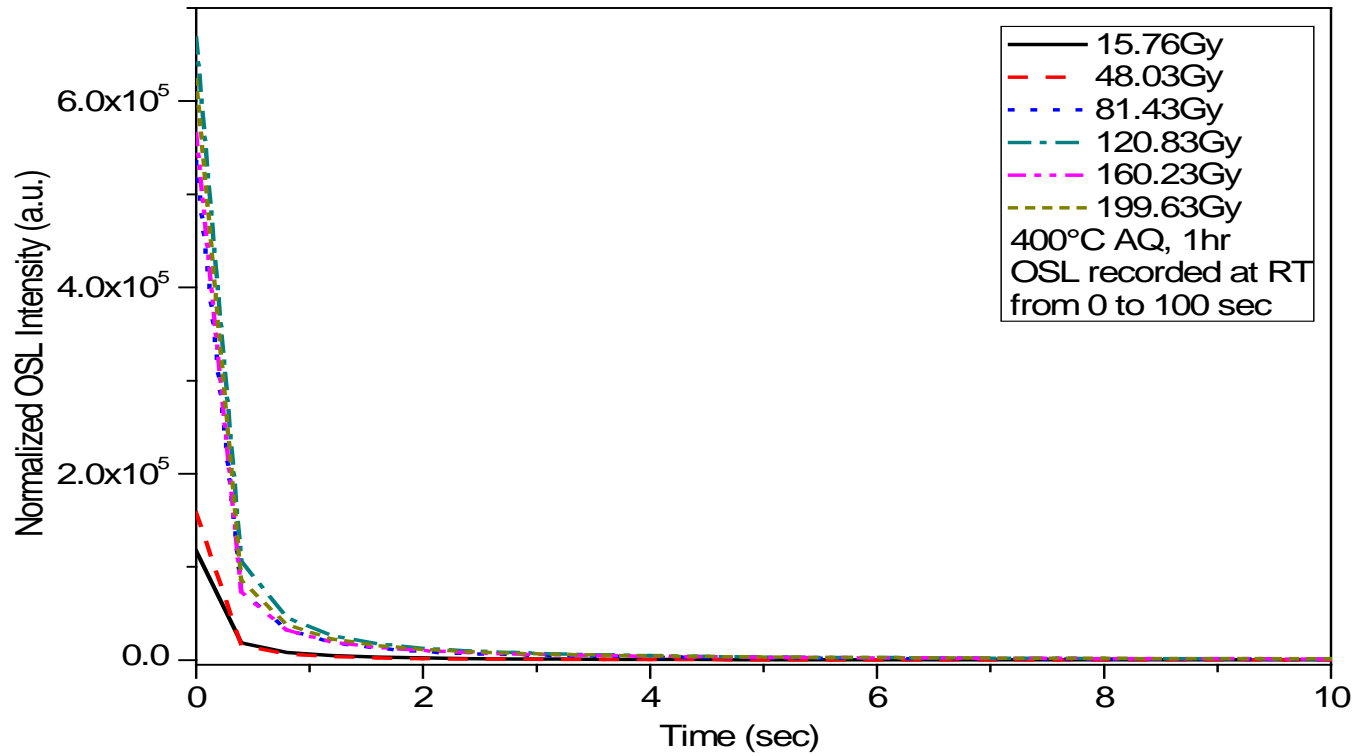
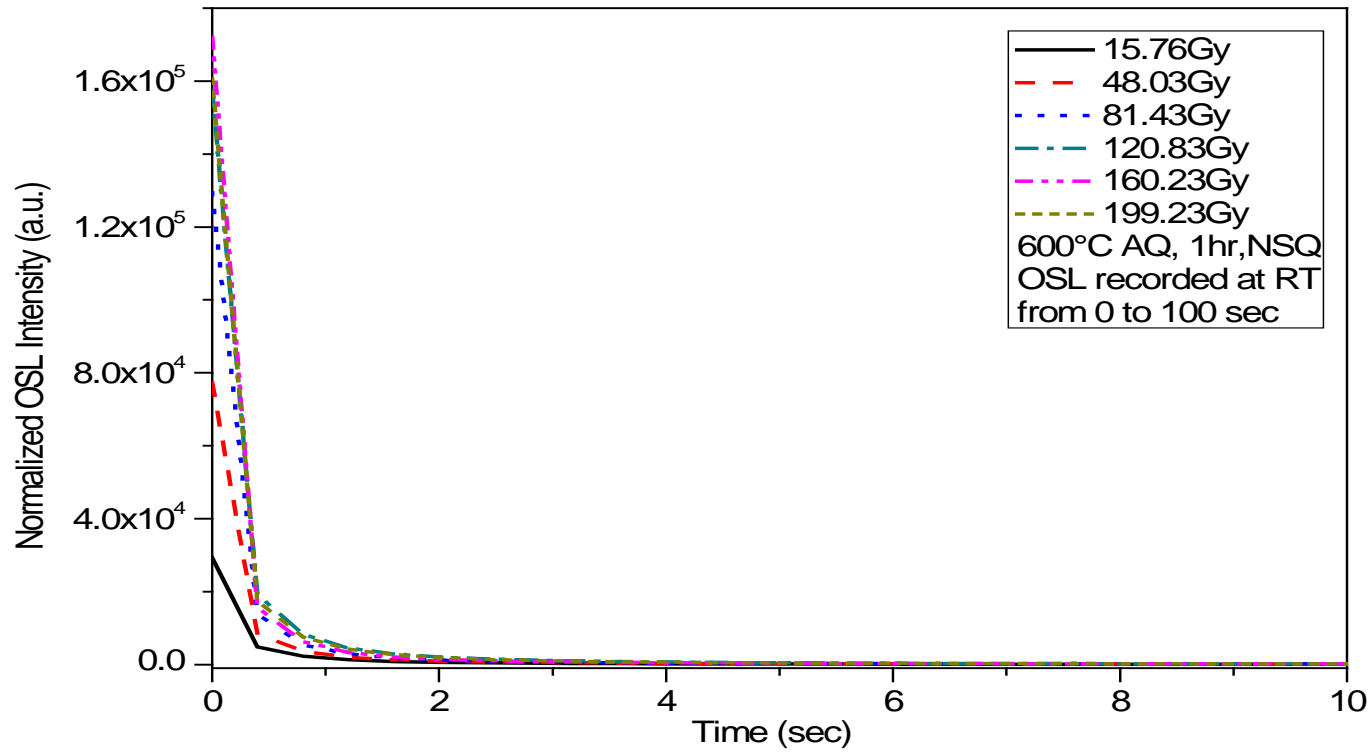
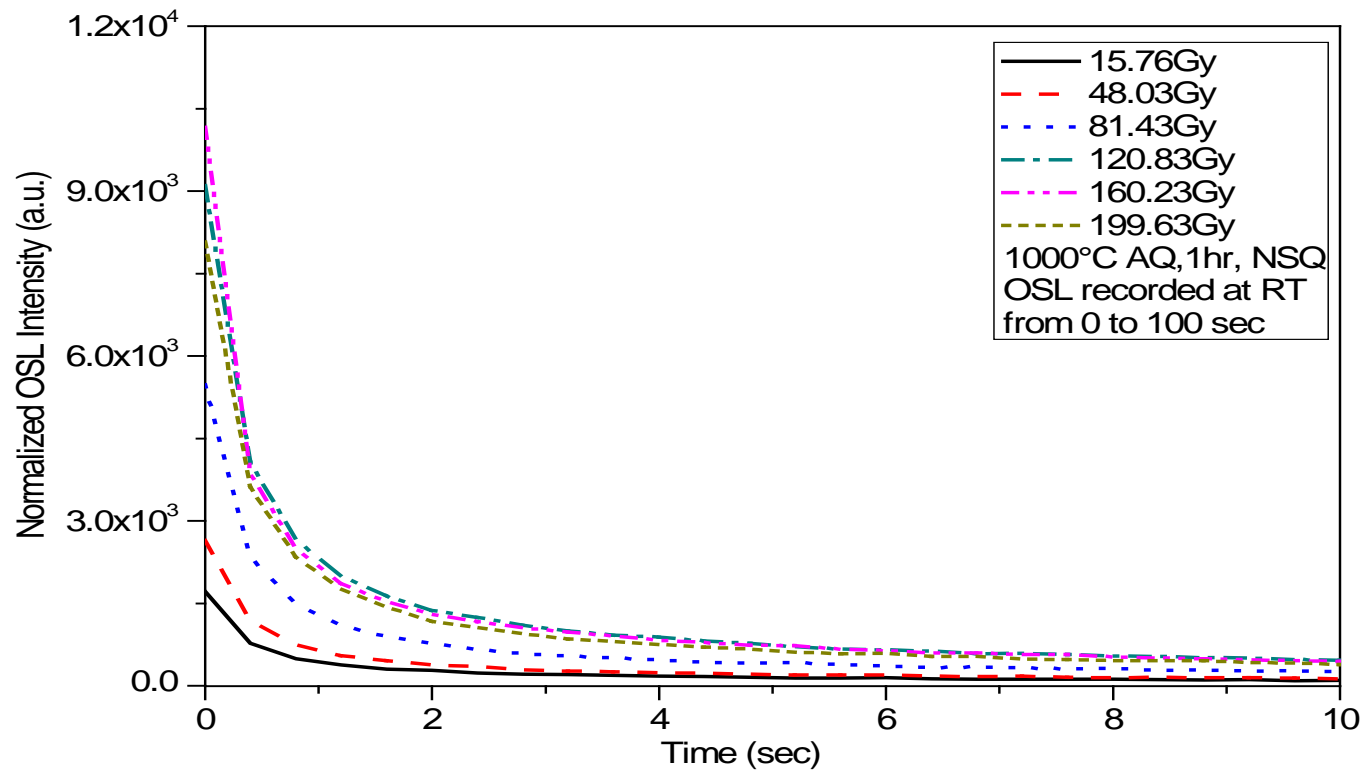


Fig. 5.13 OSL Decay curve of 400°C annealed NSQ at RT for different beta doses.



**Fig. 5.14** OSL Decay curve of 600°C annealed NSQ at RT for different beta doses.



**Fig. 5.15** OSL Decay curve of 1000°C annealed NSQ at RT for different beta doses.

Botter Jensen et al worked on OSL sensitivity of micron sized quartz samples with respect to anneal temperature up to 600°C<sup>31</sup>. They explained that phase transformation of quartz played an important role in changes of OSL sensitivity of quartz. These types of changes are described by mechanism in which alterations in the recombination center concentration is involved. Kale et al also observed similar OSL sensitivity of micron sized synthetic quartz at different annealing temperature (400°C, 600°C, 1000°C) and found that OSL sensitivity increases with rise in annealing temperature<sup>32</sup>. They also suggested that phase change was responsible for the rise of OSL sensitivity. Nandlkumar et al worked on TL and OSL of nano-crystalline K<sub>2</sub>Ca<sub>2</sub>(SO<sub>4</sub>)<sub>3</sub>:Cu phosphor annealed at different temperatures (400–900°C) for 2 hours and found that the sample annealed at 700°C was most sensitive than other annealed samples<sup>33</sup>. The 600°C and 1000°C annealed samples gave better uniform OSL growth response with beta doses up to 160.23Gy than OSL growth response with beta doses in same range for 400°C annealed samples. The strength of OSL counts decreases with rise in annealing temperature followed by identical beta doses.

#### **5.4 Comparative OSL at RT study of NSQ samples.**

The comparative studied of OSL outcomes at room temperature have been carried out under influence of (i) beta dose(s) (ii) annealing temperature(s). These studies may resolve appropriate physical treatment for better OSL outcomes which is responsible for significant contribution of OSL components in luminescence process.

##### **5.4.1 Comparative study of OSL recorded at RT between unannealed and annealed NSQ samples for beta doses.**

The annealed samples followed by beta exposures showed noticeable OSL growth over the OSL growth of unannealed samples. The patterns of rapid OSL decay within 0 to 0.4 seconds of stimulation and usual OSL decay within 0.4 to 100 seconds were found identical. The 400°C annealed samples shows average 95.36% of growth in OSL counts over unannealed samples. But, higher annealed samples exhibited lower percentages of growth in OSL counts over lower annealed samples (**Fig. 5.16**). The 400°C annealed samples

followed by beta exposures showed noticeable growth in OSL compared to unannealed samples as well as 600°C and 1000°C annealed samples.

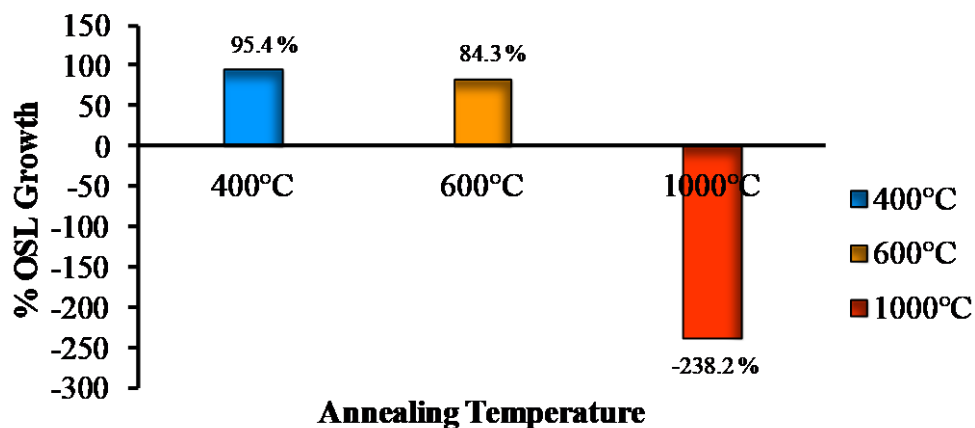


**Fig. 5.16** Average OSL growth percentage (at RT) of NSQ sample annealed at 400°C, 600°C and 1000°C w.r.t. unannealed sample.

### 5.5 Deconvolution study of OSL at RT for NSQ samples.

As per the earlier discussion, over the shape of OSL decay curves under the influence of given physical conditions to the sample and stimulation temperature the multiple complexity of OSL decay curve needs to be resolved. The shape of OSL decay curves either exponential or non-exponential reflected the contribution percentage of shallow unstable traps and optically sensitive traps. Several scientists worked on these issues and resolved these difficulties with the help of mathematical OSL deconvolution process<sup>34</sup>. It was noticed that the usual OSL decay pattern within 0.4 to 100 seconds of stimulation which is the result of multiple component of OSL decay curve. Bailey et al reported that in many samples of quartz, three main components have been observed and are informally called the fast, medium and slow components<sup>35</sup>. The contribution of proposed OSL components was considered for dating and dosimetry applications. In view of this, the attempt had been made to resolve the OSL components of NSQ samples for usual OSL decay portion within 0.4 seconds to 100 seconds of stimulations with the help of ORIGIN8 commercial software. The resolution of OSL components for NSQ sample may give significant information about fast (FC), medium (MC) and slow (SC) components of OSL

decay curves. Their contribution percentage in complex OSL decay may help to establish the correction with TL glow peaks of NSQ samples.

**5.5.1 Deconvolution study of unannealed NSQ samples of OSL at RT under the influence of beta doses.**

In chosen protocols, the maximum OSL counts were decreased very rapidly within 0 and 0.4seconds of stimulation time. Therefore, the loss of OSL counts represented a straight line over OSL against time plot with negative slope value. The partial OSL counts were decreased in typical pattern of OSL decay over 0.4 seconds to 100 seconds of stimulation. It was noticed that the OSL curves pattern was not standard exponential in shape. Therefore, OSL decay curve was de-convoluted for two sections separately between (i) 0 to 0.4seconds of stimulation and (ii) 0.4 seconds to 100 seconds of stimulation. It was found that during the optical stimulation from 0 to 0.4seconds, the average 78.21% of OSL counts were decreased very rapidly whereas the average 21.78% of OSL counts were decreased during 0.4 seconds to 100 seconds of stimulation as a usual exponential nature in unannealed NSQ sample (**Table 5.12**).

**Table 5.12** Observation of OSL (at RT and 160°C) within 0 to 0.4 seconds stimulation time for unannealed sample.

Sr. No.	Beta Dose (Gy)	OSL Intensity for Stimulation time 0.0 and 0.4 sec		Average OSL Loss (%)		Slope (k)	
		at RT	at 160°C	at RT	at 160°C	at RT	at 160°C
		1	15.76	4570.2- 322.2	4569.8 - 194	92.94	96.75
2	48.03	14924.4- 925.4	12381.8 - 567.2	93.79	95.41	-34997.5	-29536.5
3	81.43	32106.2-1786.2	25233.4 - 749	94.43	97.03	-75800	-61211
4	120.83	42177.8 - 2306.4	33981.6 - 1001.6	94.53	97.05	-99678.5	-82450
5	160.23	4763.8 - 2592.6	901 - 340.4	45.57	62.21	-5428	-1401.5
6	199.63	8182.2 - 4252.4	3121.4 - 1856	48.02	40.44	-9824.5	-3156
		<b>Mean</b>		<b>78.21</b>	<b>81.31</b>		

The earlier discussion regarding components of OSL decay demonstrated that the unannealed NSQ samples exhibited predominant contribution ultra-fast components (UFC) was related to unstable shallow trap in the material. Kale Y D elaborated the correlation between shallow traps and 110°C TL glow

peaks<sup>13</sup>. The ESR study of NSQ samples also confirm the correlation between 110°C TL glow peaks and contribution of E<sub>1</sub>' centers.

Unannealed NSQ sample explained the 78.21% of OSL loss as a rapid decay within 0 to 0.4sec of stimulation and 21.78% of OSL loss as a usual decay within 0.4 to 100s seconds of stimulations.

In continuation of current work, the nature of OSL decay components (fast, medium and slow) had been resolved for the usual exponential shape of OSL decay curves within 0.4seconds to 100seconds of optical stimulation under influence of radiation below and above 120.83Gy of beta doses for unannealed NSQ samples. For this determination, first order exponential equation;

$$y = A1 * \exp\left(\frac{-x}{t_1}\right) + A2 * \exp\left(\frac{-x}{t_2}\right) + A3 * \exp\left(\frac{-x}{t_3}\right) + y_0$$

was fitted to proposed exponential shape of decay curve by ORIGIN8 commercial software. The output of equation represented y as Intensity, x as stimulation time, A1, A2 and A3 as amplitudes, t<sub>1</sub>, t<sub>2</sub> and t<sub>3</sub> as time required for electrons to recombine with hole at recombination center whereas reciprocal of t<sub>1</sub>, t<sub>2</sub> and t<sub>3</sub> represented the value of decay constant. It was denoted by (f) or (λ). Offset intensity was represented as y<sub>0</sub>. These studies may support to analyse and decide the (i) nature (fast, medium and slow) of decay of optically sensitive traps (ii) contribution percentage of or involvement of the components in OSL decay curve and (iii) dual nature of traps and therefore establish the correlation between TL and OSL.

During optical stimulation from 0.4 second to 100 seconds, the usual OSL decay pattern was resolved by fitting of identical exponential equation. The OSL outcome showed 20.53% contribution from fast component (FC), 35.11% of contributions from medium component (MC) and 44.35% of contribution from slow component (SC) (**Table 5.13**). Thus, un-annealed sample followed by beta doses exhibited predominant contribution of slow components by 44.35%.

In OSL process, the role of photoionization cross-section (PIC) is very essential to be considered. It can explain whether particular trap is optically sensitive/active or not and whether all TL traps involved optically active or not. These questions can be answered by smaller or larger values of PIC at a given stimulation wavelength. The photoionization cross-section (PIC) represents

how stimulation light interacts with the electron trapped in the potential well, so that it can be released optically. The PIC area have calculated for fast, medium and slow components of OSL decay curves under influence of total beta doses. For this calculation, well defined equation of photoionization cross-section (PIC) was used<sup>34</sup>.

$$f = (\sigma_p) \left( \frac{I}{h\nu} \right)$$

Where;  $f$  is decay constant in *second*<sup>-1</sup>,  $\sigma_p$  is photoionization cross section in *meter*<sup>2</sup>,  $I$  is Intensity of optical stimulation light in *Watt per meter*<sup>2</sup>,  $h$  is Plank Constant in *joule-seconds* and  $\nu$  is frequency of optical stimulation light in *hertz*. Re-arrange the equation and hence the photoionization cross-section (PIC) had been calculated by

$$\sigma_p = \left( \frac{hc}{\lambda} \right) (f)$$

Where;  $\nu = c/\lambda$  and  $c$  is speed of light in *meter per second* and  $\lambda$  is wavelength of optical stimulation light in *meter*.

These outcomes presented the knowledge of contribution of OSL components and it was represented by photo ionised cross-sectional area where optically sensitized charges were accumulated. Under this protocol, the fast component (FC) of OSL decay curve had larger photo ionization cross-section area than photo ionization cross-section area of medium and slow components (MC and SC), however, it displayed lower percentage of contribution than medium and slow components (**Table 5.14**). Therefore, it is unambiguously pointed out that the OSL components percentage does not depend upon the area of the PIC but depends upon the accumulation of the concentration of optically sensitized charges in the sample. Unannealed samples followed by beta doses exhibited fast and medium components of OSL which is suggestive of higher photoionization cross section over the PIC of slower components of OSL.

**Table 5.13** OSL components (at RT and at 160°C) of unannealed sample for 0.4 and 100sec of stimulation time.

Sr. No.	Beta Dose (Gy)	OSL Intensity for Stimulation Time 0.4sec to 100sec		Average OSL Loss (%)		Average Fast Components (%)		Average Medium Components (%)		Average Slow Components (%)	
		at RT	at 160°C	at RT	at 160°C	at RT	at 160°C	at RT	at 160°C	at RT	at 160°C
1	15.76	322.2	194	7.06	3.25	20.79	35.38	46.37	17.94	32.84	46.68
2	48.03	925.4	567.2	6.21	4.59	16.91	34.06	49.84	27.24	33.25	38.70
3	81.43	1786.2	749	5.57	2.97	43.34	24.52	29.88	32.36	26.78	43.12
4	120.83	2306.4	1001.6	5.47	2.95	28.08	31.74	41.87	28.21	30.05	40.05
5	160.23	2592.6	340.4	54.43	37.79	7.80	5.17	23.79	29.75	68.41	65.08
6	199.63	4252.4	1859	51.98	59.56	6.27	9.22	18.92	37.03	74.81	53.75
<b>Mean</b>				<b>21.78</b>	<b>18.68</b>	<b>20.53</b>	<b>35.02</b>	<b>35.11</b>	<b>28.75</b>	<b>44.35</b>	<b>47.89</b>

**Table 5.14** PIC of OSL (at RT and at 160°C) of unannealed sample for 0.4 to 100sec of stimulation time.

Sr. No.	Beta Dose (Gy)	Stimulation Time (sec)	Avg. $\sigma$ Fast Components		Avg. $\sigma$ Medium Components		Avg. $\sigma$ Slow Components	
			at RT	at 160°C	at RT	at 160°C	at RT	at 160°C
1	15.76	0.4 - 100	76.162 E-22	99.470 E-22	14.052 E-22	12.00 E-22	1.454 E-22	1.884 E-22
2	48.03	0.4 - 100	73.829 E-22	64.038 E-22	19.818 E-22	11.18 E-22	1.961 E-22	0.993 E-22
3	81.43	0.4 - 100	41.542 E-22	79.375 E-22	8.463 E-22	13.92 E-22	0.930 E-22	1.197 E-22
4	120.83	0.4 - 100	56.733 E-22	55.081 E-22	11.295 E-22	6.755 E-22	1.369 E-22	0.822 E-22
5	160.23	0.4 - 100	22.777 E-22	21.032 E-22	4.700 E-22	4.185 E-22	0.778 E-22	0.664 E-22
6	199.63	0.4 - 100	32.568 E-22	16.259 E-22	6.764 E-22	3.490 E-22	0.845 E-22	0.649 E-22
<b>Mean</b>			<b>50.603 E-22</b>	<b>55.876 E-22</b>	<b>10.849 E-22</b>	<b>8.588 E-22</b>	<b>1.222 E-22</b>	<b>1.034 E-22</b>

### 5.5.2 Deconvolution study of annealed NSQ samples of OSL at RT under the influence of beta doses.

OSL recorded at RT of thermally treated NSQ samples under the influence of beta doses are being also considered for deconvolution study in line with earlier studies for untreated specimens. The 400°C annealed samples followed by identical beta doses exhibited loss of OSL counts by average 86.33% as a rapid decay. These losses of OSL counts raise little by average 88.33% as a rapid decay in 600°C annealed sample. But, 1000°C annealing treatment gave loss of OSL counts by average 56.66% as a rapid decay within 0 to 0.4seconds of stimulation (**Fig. 5.17**).

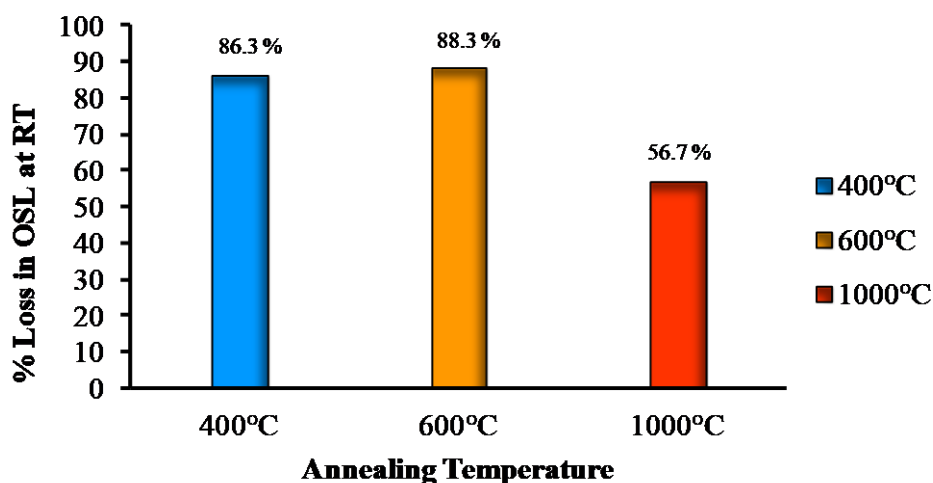


**Fig. 5.17** Observation for average percentage loss in OSL at RT within 0 to 0.4 seconds stimulation time for NSQ samples annealed at 400°C, 600°C and 1000°C.

As a usual OSL decay, higher annealed sample offered average 43.33% of OSL losses within 0.4 to 100seconds of stimulation. It is indicative that a higher annealing treatment supports the increase in the usual part of the OSL decay component by reducing the losses of OSL counts as UFC of OSL decay. This supports to resolve the responsible components of OSL decay curve. The lower annealed samples being annealed at 400°C and 600°C seems to increase medium components of OSL decay within 0.4 to 100 seconds of stimulation from average 40.78% to average 43.93%, whereas this contribution decreases by average 28.65% in higher annealed sample of 1000°C. The higher annealed

samples also showed increase in the contribution of slower components by average 59.40% in usual OSL decay (**Table 5.15**).

It was further found that for lower annealed samples, the photoionization cross section for fast component of OSL was higher than the medium and slow components of OSL. This pattern of process sustained even for higher annealed samples (**Table 5.16**).

It is reasonable to understand that the higher annealing treatment supports the increase in the contribution of usual components outcomes controlling the losses of OSL counts as a rapid decay at RT as well at 160°C (**Fig. 5.18, Fig. 5.19**). It is discernible to note that the lower annealed samples supported contribution of medium components of OSL while the higher annealed samples supported to increase the contribution of slower components. Here also, the photoionization cross section of fast component of OSL was higher than PIC of medium and slow components of OSL.

While comparing deconvolution observations between unannealed and annealed NSQ samples for beta doses interesting observations were brought out. The lower annealed samples enhanced the contribution of fast and medium components of OSL over components of unannealed samples within 0.4 to 100 seconds of stimulation. The contributions of proposed components were diminished by the growth of slower components of OSL in higher annealed samples over unannealed samples (**Table 5.13, Table 5.15**).

The lower annealed samples enhanced the PIC of fast and medium components of OSL decay curves over PIC of unannealed samples (**Table 5.14, Table 5.16**).

**Table 5.15** OSL components (at RT and at 160°C) of annealed sample for 0.4 and 100sec of stimulation time.

Sr. No.	Sample Description	Beta Dose (Gy)	Stimulation Time (sec)	Average OSL Loss (%)		Average Fast Component (%)		Average Medium Component (%)		Average Slow Component (%)	
				at RT	at 160°C	at RT	at 160°C	at RT	at 160°C	at RT	at 160°C
1	NSQ Annealed at 400°C, 1Hr	15.76	0.4 - 100	15.84	11.18	28.92	22.85	45.23	33.57	25.85	43.58
2		48.03	0.4 - 100	9.78	7.74	29.21	17.45	39.98	52.43	30.81	30.12
3		81.43	0.4 - 100	13.86	10.51	28.64	19.30	40.55	42.63	30.80	38.07
4		120.83	0.4 - 100	15.85	8.49	29.32	24.22	41.13	45.40	29.55	30.38
5		160.23	0.4 - 100	12.92	9.62	26.55	26.87	38.16	50.10	35.29	23.03
6		199.63	0.4 - 100	13.77	13.95	27.40	20.41	39.65	56.77	32.95	22.82
Mean				<b>13.67</b>	<b>10.24</b>	<b>28.34</b>	<b>21.85</b>	<b>40.78</b>	<b>46.81</b>	<b>30.87</b>	<b>31.33</b>
7	NSQ Annealed at 600°C, 1Hr	15.76	0.4 - 100	16.47	5.63	28.88	15.39	48.49	54.98	22.63	29.63
8		48.03	0.4 - 100	10.89	6.26	36.39	36.64	41.35	36.73	22.26	23.63
9		81.43	0.4 - 100	10.66	2.69	33.85	20.71	45.44	24.70	20.70	54.60
10		120.83	0.4 - 100	12.21	4.5	36.21	21.57	42.65	43.03	21.14	35.40
11		160.23	0.4 - 100	9.09	3.23	37.89	24.17	41.72	31.97	20.39	43.86
12		199.63	0.4 - 100	10.83	4.65	33.54	26.82	43.94	35.73	22.52	37.45
Mean				<b>11.69</b>	<b>4.49</b>	<b>34.46</b>	<b>24.21</b>	<b>43.93</b>	<b>37.85</b>	<b>21.60</b>	<b>37.42</b>
13	NSQ Annealed at 1000°C, 1Hr	15.76	0.4 - 100	45.21	65.39	9.95	5.91	26.96	23.61	63.09	70.48
14		48.03	0.4 - 100	44.69	61.68	11.80	5.57	26.33	21.21	61.87	73.22
15		81.43	0.4 - 100	42.75	60.29	12.71	5.18	27.81	23.03	59.48	71.79
16		120.83	0.4 - 100	44.68	62.30	12.24	6.36	29.81	22.67	57.95	70.97
17		160.23	0.4 - 100	37.97	46.41	11.82	4.99	30.57	19.95	57.61	75.06
18		199.63	0.4 - 100	44.73	60.44	13.11	6.26	30.46	21.40	56.43	72.34
Mean				<b>43.33</b>	<b>59.41</b>	<b>11.93</b>	<b>5.71</b>	<b>28.65</b>	<b>21.97</b>	<b>59.40</b>	<b>72.31</b>

**Table 5.16** PIC of OSL (at RT and at 160°C) of annealed sample for 0.4 to 100sec of stimulation time.

400AQ								
Sr. No.	Beta Dose (Gy)	Stimulation Time (sec)	Avg. $\sigma$ Fast Components		Avg. $\sigma$ Medium Component		Avg. $\sigma$ Slow Components	
			at RT	at 160°C	at RT	at 160°C	at RT	at 160°C
1	15.76	0.4 - 100	57.899 E-22	44.973 E-22	15.810 E-22	10.668 E-22	2.959 E-22	1.122 E-22
2	48.03	0.4 - 100	63.564 E-22	121.654 E-22	17.079 E-22	19.754 E-22	3.195 E-22	1.462 E-22
3	81.43	0.4 - 100	59.540 E-22	59.752 E-22	14.897 E-22	16.369 E-22	2.621 E-22	1.155 E-22
4	120.83	0.4 - 100	60.165 E-22	60.392 E-22	14.136 E-22	14.846 E-22	2.181 E-22	1.302 E-22
5	160.23	0.4 - 100	58.512 E-22	60.392 E-22	12.609 E-22	15.017 E-22	2.009 E-22	1.538 E-22
6	199.63	0.4 - 100	58.102 E-22	51.087 E-22	12.750 E-22	14.391 E-22	1.843 E-22	2.754 E-22
<b>Mean</b>			<b>59.630 E-22</b>	<b>66.375 E-22</b>	<b>14.547 E-22</b>	<b>15.174E-22</b>	<b>2.468 E-22</b>	<b>1.555 E-22</b>
600 AQ								
1	15.76	0.4 - 100	53.682 E-22	110.522 E-22	16.481 E-22	18.989 E-22	3.153 E-22	2.295 E-22
2	48.03	0.4 - 100	53.512 E-22	56.179 E-22	12.791 E-22	15.125 E-22	2.021 E-22	1.551 E-22
3	81.43	0.4 - 100	66.313 E-22	60.827 E-22	17.951 E-22	10.839 E-22	2.542 E-22	0.893 E-22
4	120.83	0.4 - 100	54.548 E-22	96.628 E-22	14.502 E-22	17.415 E-22	2.426 E-22	2.308 E-22
5	160.23	0.4 - 100	58.310 E-22	59.752 E-22	15.528 E-22	10.621 E-22	2.260 E-22	0.843 E-22
6	199.63	0.4 - 100	56.361 E-22	62.862 E-22	15.165 E-22	13.452 E-22	2.577 E-22	1.057 E-22
<b>Mean</b>			<b>57.122 E-22</b>	<b>74.462 E-22</b>	<b>15.403 E-22</b>	<b>14.407E-22</b>	<b>2.496 E-22</b>	<b>1.491 E-22</b>
1000AQ								
1	15.76	0.4 - 100	39.053 E-22	20.596 E-22	6.385 E-22	5.155 E-22	0.941 E-22	0.539 E-22
2	48.03	0.4 - 100	35.525 E-22	21.459 E-22	5.985 E-22	4.590 E-22	0.828 E-22	0.370 E-22
3	81.43	0.4 - 100	33.222 E-22	22.975 E-22	5.371 E-22	5.142 E-22	0.829 E-22	0.419 E-22
4	120.83	0.4 - 100	31.785 E-22	19.731 E-22	5.107 E-22	4.441 E-22	0.848 E-22	0.459 E-22
5	160.23	0.4 - 100	32.771 E-22	23.101 E-22	4.718 E-22	5.349 E-22	0.763 E-22	0.448 E-22
6	199.63	0.4 - 100	30.578 E-22	20.083 E-22	4.717 E-22	4.244 E-22	0.760 E-22	0.387 E-22
<b>Mean</b>			<b>33.822 E-22</b>	<b>21.324 E-22</b>	<b>5.380 E-22</b>	<b>4.820 E-22</b>	<b>0.828 E-22</b>	<b>0.437 E-22</b>

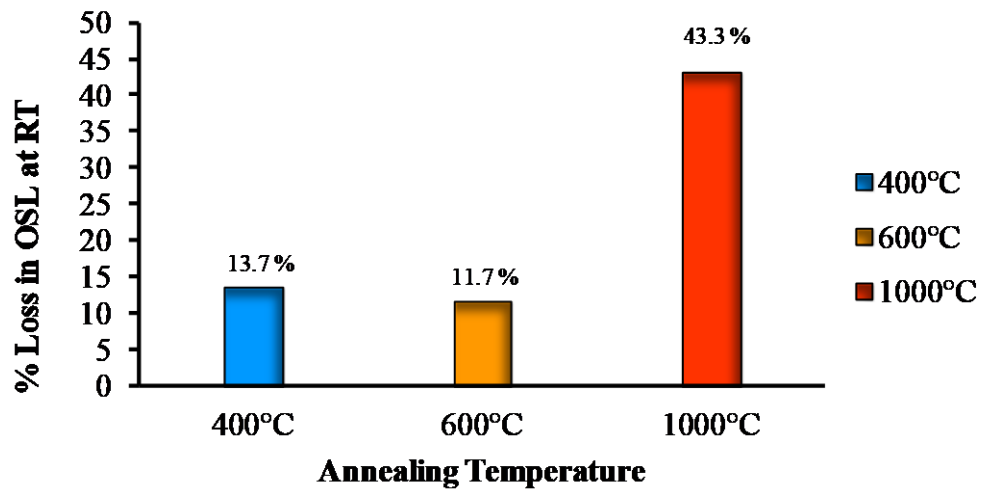


**Fig. 5.18** Observation for average percentage loss in OSL at RT within 0.4 to 100 seconds stimulation time for samples annealed at 400°C, 600°C and 1000°C.

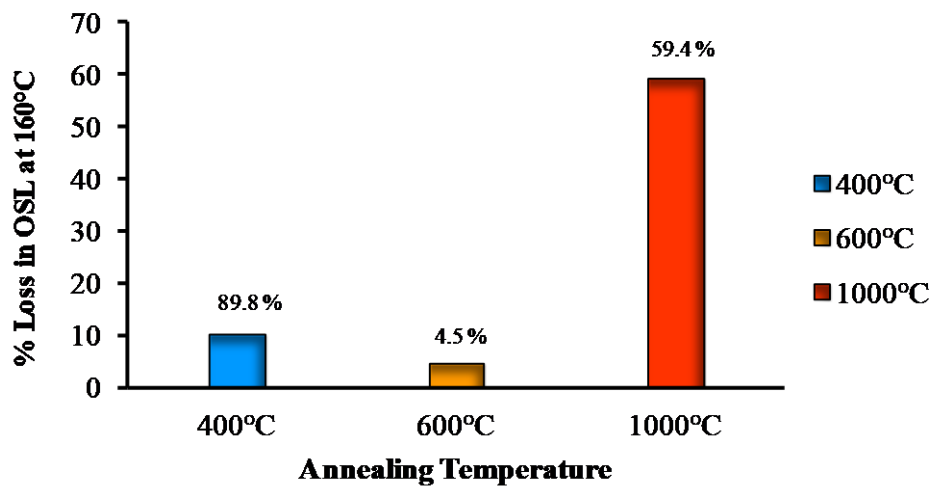


**Fig. 5.19** Observation for average percentage loss in OSL at 160°C within 0.4 to 100 seconds stimulation time for samples annealed at 400°C, 600°C and 1000°C.

### 5.6 OSL at RT-DRC study for NSQ samples.

The characteristics of OSL dose response under stimulation at room temperature was represented by the log (OSL-Intensity) verses log (Dose) scale. The slope value is calculated by relation between OSL and Dose i.e

$$OSL\ Intensity = a.D^k$$

Where  $a$  is constant,  $D$  is applied dose,  $k$  value is related to slope of the DRC and it represents if  $k > 1$ ; for superlinear,  $k = 1$ ; for linear and  $k < 1$ ; for sublinear<sup>21</sup>.

#### 5.6.1 OSL at RT-DRC study of unannealed NSQ samples.

To understand the OSL sensitivity response of the sample with applied beta radiation doses, the OSL decay curves were recorded at room temperature for different beta exposures. The unannealed samples displayed systematic growth in OSL intensity from 4570.2counts to 42177.8counts under influence of 15.76Gy, 48.03Gy, 81.43Gy and 120.83Gy beta doses. Further rise in beta doses, the variations in OSL intensity was also observed in the sample. In this part of work, the slope value ( $k$ ) of OSL dose response was observed by 1.12 which reveals super-linear characteristics of OSL dose response for unannealed sample (Table 5.17).

**Table 5.17** Observation of OSL-DRC (at RT) of Unannealed, 400°C, 600°C and 1000°C annealed NSQ samples at (15.76Gy-199.6Gy) beta dose.

Sr. No.	Sample description	Slope (k)	Nature of Dose Response Curve
1	Un-annealed	1.12	Supra-linear
2	400°C Annealed	0.75	Sub-linear
3	600°C Annealed	0.79	Sub-linear
4	1000°C Annealed	0.81	Sub-linear

#### 5.6.2 OSL at RT-DRC study of annealed NSQ samples.

In order to investigate, the effects of annealing temperature on OSL-DRC curves were studied under influence of various doses. The nature of OSL-DRC curve was defined by the calculating  $k$  value i.e. slope of the DRC. It was observed that 600°C and 1000°C annealed samples showed systematic growth of OSL counts with rise in beta dose up to 160.23Gy of radiations. Thereafter, the identical annealed samples showed variations in OSL response. The

variations in OSL at RT DRC response was considered up to 120.83Gy of radiations in 400°C annealed samples. The changes in OSL dose response curves under influence of annealing treatment gave  $k$  value below unity and hence it is suggested as the sub-linear nature of OSL dose response curve of annealed samples (**Table 5.17**). The annealing treatments offered significant rise in OSL counts for annealed NSQ samples than unannealed samples. The lower annealing temperatures helped to enhance better OSL strength in annealed samples than higher annealing temperature. Also, annealing treatments changed the super-linear nature of OSL DRC into sub-linear nature of OSL DRC for NSQ samples (**Table 5.17**)

McKeever S et al. explained super-linear and sub-linear behaviour of OSL DRC with the help of different models<sup>17</sup>. Pagonis et al. clearly indicated the importance of competition effect between traps and centers and also explained the specific behaviour of material during excitation and read out for different OSL dose responses<sup>21</sup>. Lawless et al. as well explained the sub linear behaviour with one trap-one recombination center (OTOR) model when traps are far from saturation<sup>22</sup>.

In present work, prepared unannealed NSQ sample showed super linearity with rise in beta radiation dose which turned into sublinearity as sample annealed at different temperatures. The superlinearity of OSL DRC for unannealed NSQ sample with rise in radiation dose might be due to the competition between the trap and the recombination center for free electrons during irradiation. The shifting of superlinearity in unannealed NSQ specimens into sublinearity with thermal treatment to the NSQ specimens indicated that the competitors/electron traps may be removed or non-recombination centers might have been activated due to annealing temperature<sup>36</sup>.

### **5.7 OSL study of NSQ samples at elevated temperature (160°C ET)**

Botter-Jensen L and Kale Y D reported and explained the occurrence of unusual shape of OSL decay curves which exhibited during optical stimulation near room temperature<sup>1,13</sup>. It was established that the re-trapping of electrons by the shallow TL traps are responsible for influencing such decay curves as, quartz samples show rapid OSL decay within lower optical stimulation time say 0 to 0.4seconds. Under these optical stimulation times, the significant OSL

counts were decreased rapidly which were attributed to availability of unstable shallow traps<sup>30</sup>.

To avoid these problems, Murray A et al. have suggested elevated temperature OSL protocol<sup>37</sup>. In which, the optical stimulation is possible at specific temperature and hence this chosen specific temperature is capable enough to erase the contribution of shallow traps and unstable traps. Also, stimulation at such desired temperature helps to transfer the charges from shallow traps to optically sensitive traps and restricts to re-trapping of the optically released charges into desired temperature traps. It offers significant OSL contribution from valuable optically sensitive traps. In quartz sample, the variations in shallow TL traps under influence of physical treatments to the sample are found between 89°C to 150°C<sup>12</sup>. So, the TL glow peak within these wider ranges of temperature is known as shallow TL traps. However, the several workers have suggested that optical stimulation at 125°C temperature is sufficient to remove unstable or shallow traps<sup>20</sup>. In present work, the selection of 160°C bleaching temperature is being considered to erase sufficient quantity of unstable traps and shallow traps.

### **5.7.1 Effect of beta doses on OSL decay recorded at elevated temperature (ET) at 160°C for unannealed NSQ samples.**

The batches of unannealed NSQ samples were exposed by identical beta doses and OSL decay curves were recorded at 160°C for 100seconds of stimulation by 470nm bluish-green light. It was observed that OSL decay pattern at 160°C of stimulation was identical to the OSL decay pattern of stimulation at room temperature. Also, chosen bleaching temperature showed uniform OSL growth from 4569.8 to 33981.6 counts with beta doses up to 120.83Gy. Thereafter, the variations in OSL counts were observed with rise in beta doses (**Fig. 5.20**).

Under the influence beta doses, the unannealed NSQ samples exhibited the rapid OSL decay within 0 to 0.4 seconds and typical OSL decay within 0.4 to 100 seconds of stimulation at 160°C. The contributions of ultra-fast components (UFC) and usual OSL components (fast, medium and slow) still exist as similar to that of OSL of NSQ recorded at RT.

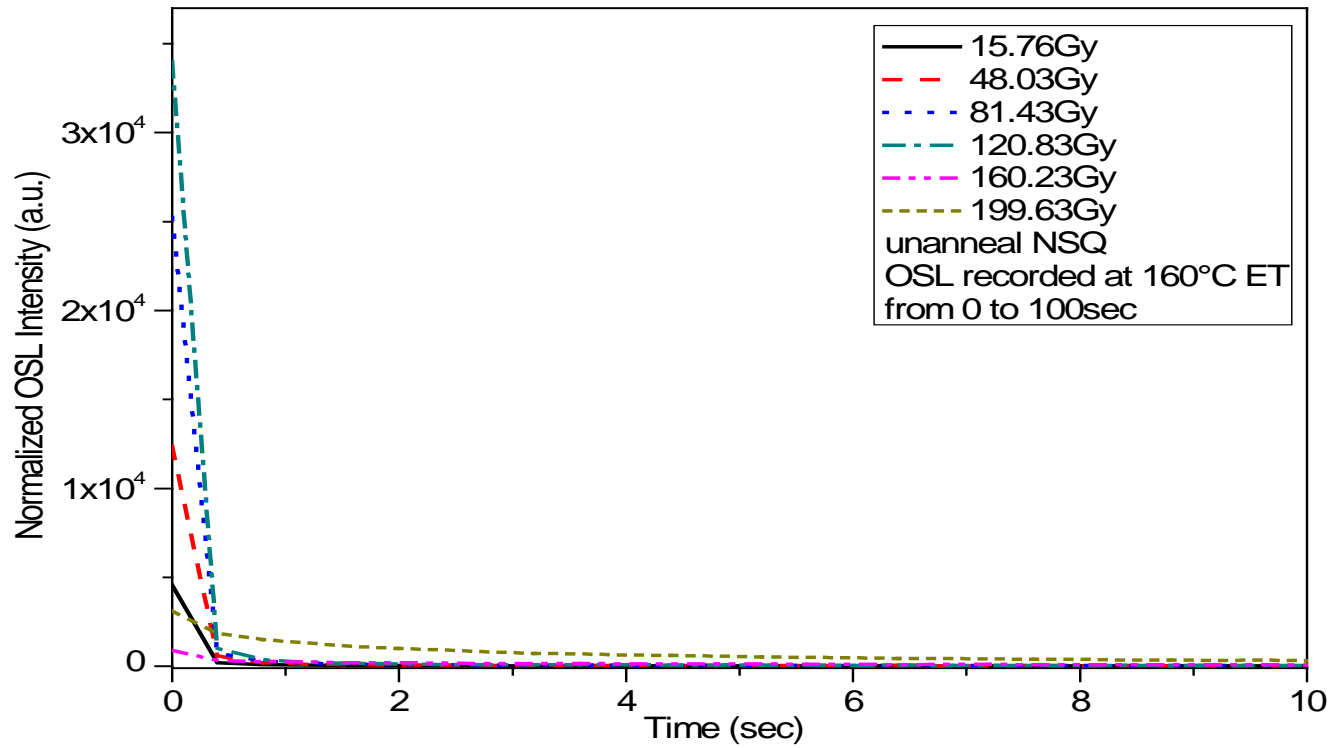


Fig. 5.20 OSL Decay curve of unannealed NSQ at 160°C ET for different beta doses.

### **5.7.2 Effect of beta dose on OSL study at 160°C ET for annealed NSQ samples**

The behaviour of UFC, usual components and the OSL intensity were being studied under effect of identical annealing treatments followed by identical beta doses. The OSL decay curves were recorded at 160°C ET and they exhibited identical pattern as similar to that of OSL decay recorded at room temperature. Optical stimulation at 160°C demonstrated the systematic OSL growth with the doses for 600°C annealed samples. Also, the strength of OSL counts in higher annealed samples was weaker than OSL strength of lower annealed samples (**Fig. 5.21, Fig. 5.22 and Fig. 5.23**).

Literature revealed that strength of OSL of micron sized synthetic quartz increases with increase in annealing temperature<sup>1,29</sup>. They suggested that the phase transformation and growth/decay of centers are responsible for increase in signal strength with annealing temperature. The present work on NSQ showed identical pattern of OSL at 160°C ET as similar pattern as obtained for OSL recorded at RT. The strength of OSL counts decreased with the rise in annealing temperature followed by identical beta doses was also observed.

The 400°C annealed sample showed an average rise of 37.61% in OSL over unannealed samples. This OSL growth further increased with annealing temperature to 600°C by average of 51% over unannealed samples. But the strength of OSL counts suddenly dropped by further rise in annealing temperature to 1000°C (**Fig. 5.24**).

The annealing temperatures from 400°C to 600°C supported the growth of OSL counts at 160°C stimulation. While, for 1000°C annealed samples the strength of OSL count significantly reduces.

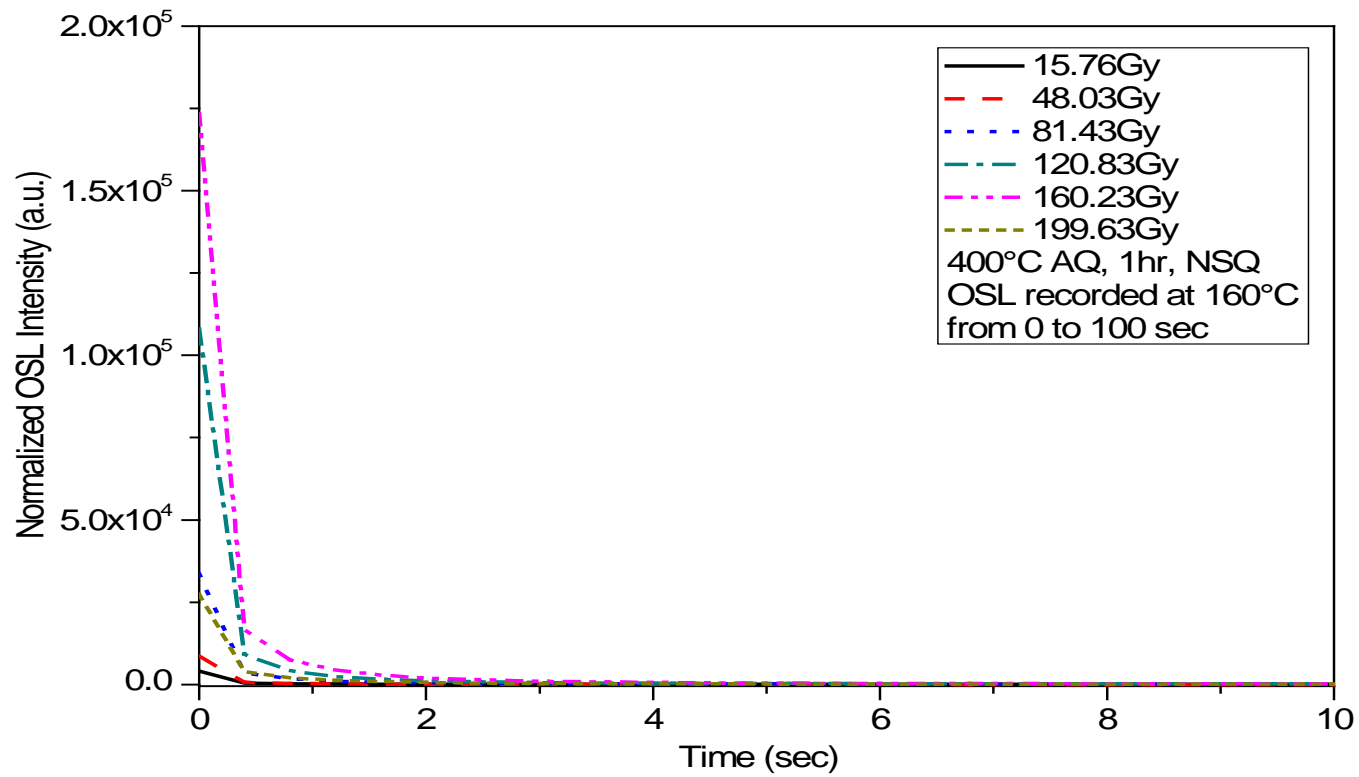


Fig. 5.21 OSL Decay curve of 400°C annealed NSQ at 160°C ET for different beta doses.

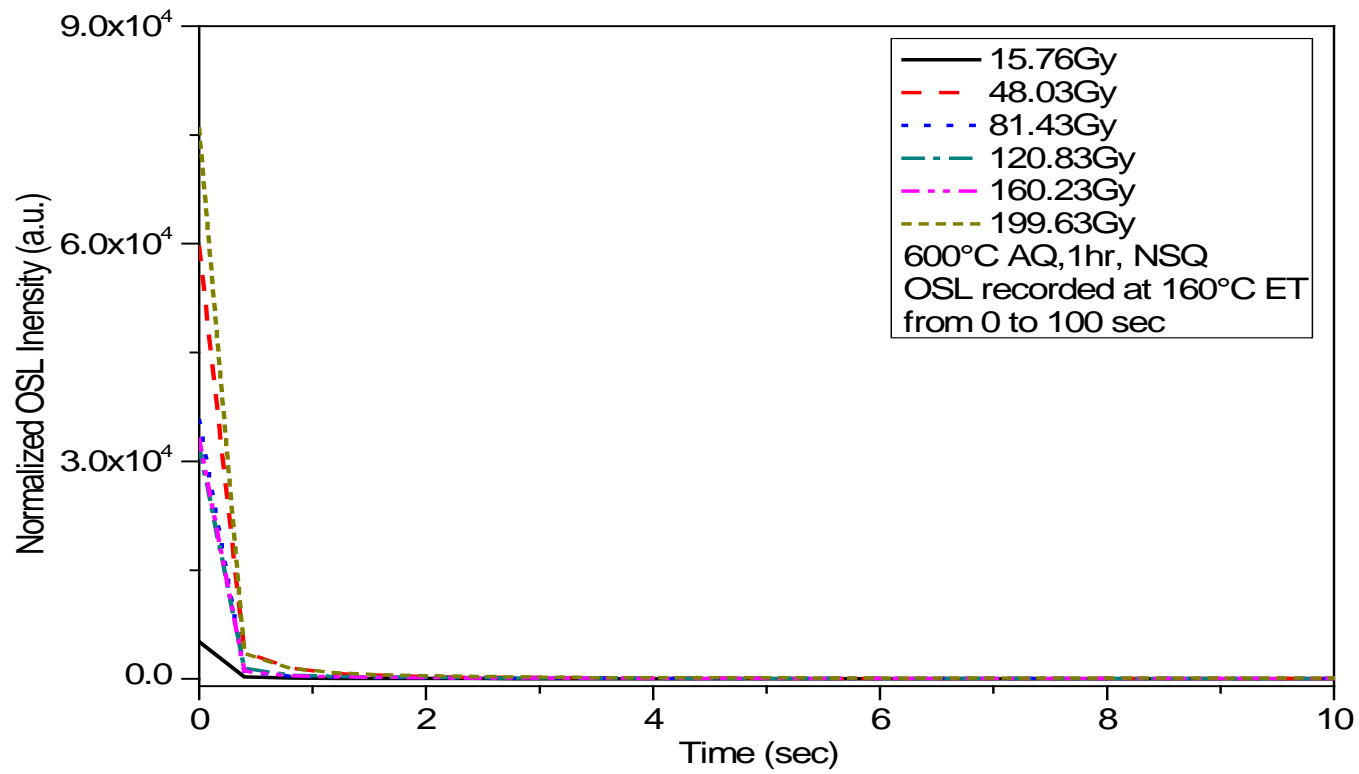
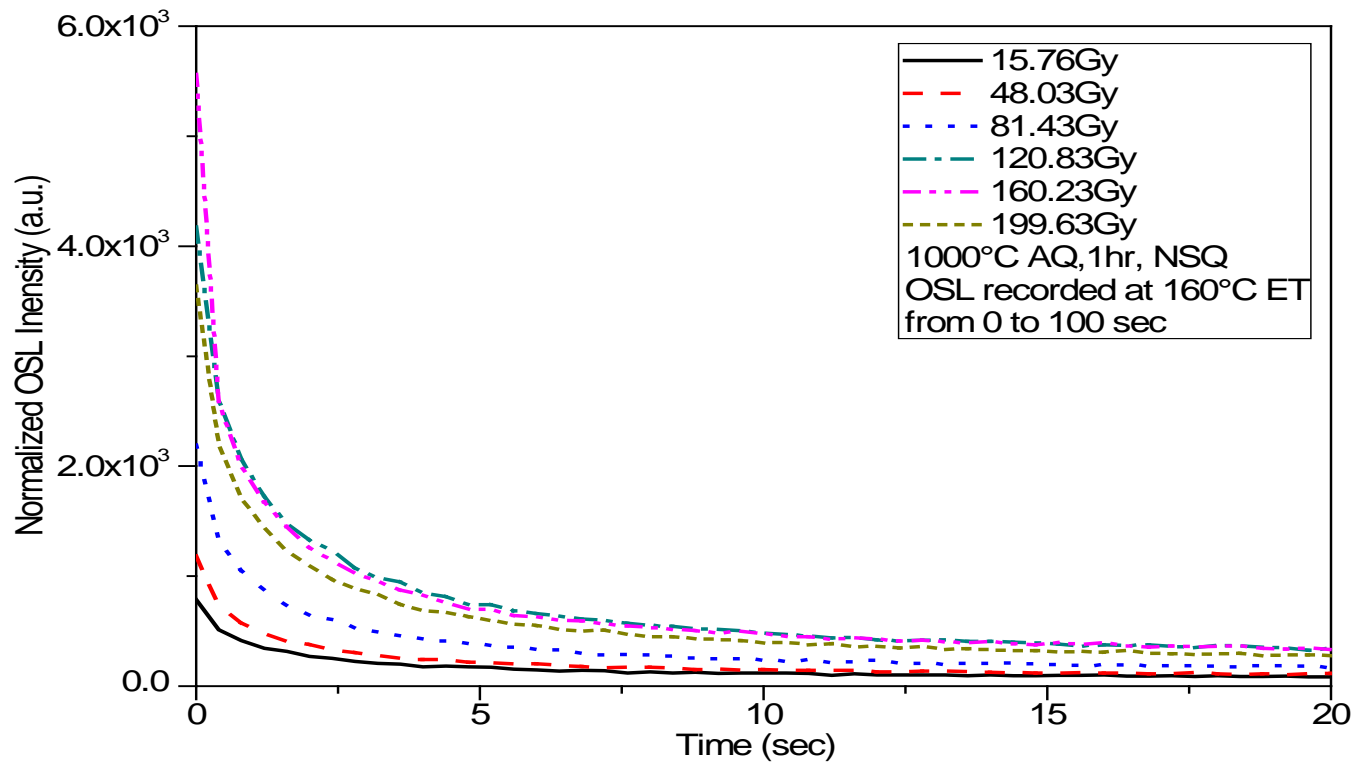
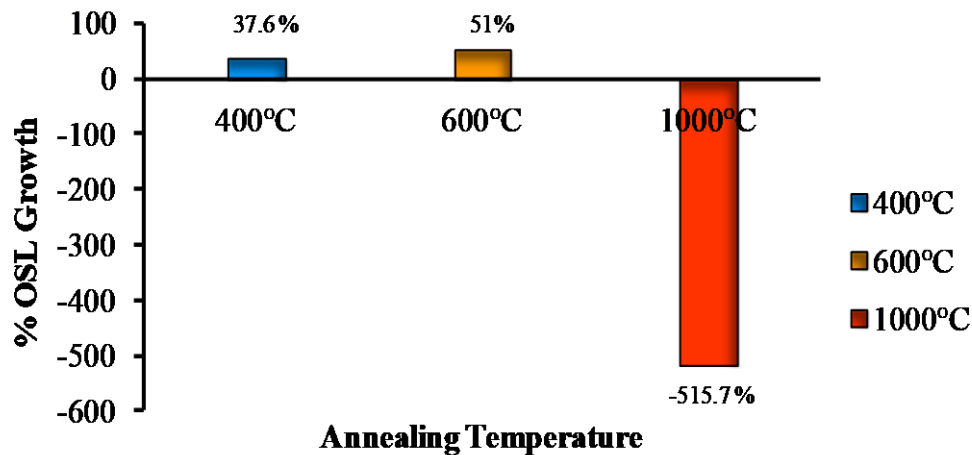


Fig. 5.22 OSL Decay curve of 600°C annealed NSQ at 160°C ET for different beta doses.



**Fig. 5.23** OSL Decay curve of prepared 1000°C annealed NSQ at 160°C ET for different beta doses.



**Fig. 5.24** Observation for average percentage OSL growth at 160°C of NSQ samples annealed at 400°C, 600°C and 1000°C w.r.t. unannealed samples.

### 5.8 Deconvolution study of OSL at ET for NSQ samples.

Like OSL at room temperature deconvolution, the OSL decay curves at 160°C were also de-convoluted under the identical physical conditions. The OSL deconvolution outcomes at elevated temperature and at room temperature were correlated.

#### 5.8.1 Deconvolution study of unannealed NSQ samples of OSL at ET under the influence of beta doses.

Under the influence of 160°C bleaching temperature, the OSL counts decreased by average 81.31% within 0 to 0.4sec of stimulation as a rapid decay and 18.68% within 0.4 to 100s seconds of stimulations as a usual OSL decay (**Fig. 5.16**).

During optical stimulation at 160°C, from 0.4 second to 100 seconds, the usual OSL decay pattern was resolved by fitting of exponential equation previously used for OSL decay at RT. From the resultant OSL outcomes, average 35.02% contribution from fast components (FC), average 28.75% of contributions from medium components (MC) and average 47.89% of contribution from slower components (SC) was observed (**Table 5.13**).

Unannealed samples followed by beta doses exhibited predominant contribution of slow components by average 47.89%.

Under present protocol, the fast components of OSL decay curve had larger photo ionization cross-section area than photo ionization cross-section area of medium and slow components. Even though, it showed lower percentage of contribution than slow components (**Table 5.14**).

Unannealed samples followed by radiation doses exhibited higher photoionization cross section of fast components than photoionization cross section fast and medium components of OSL.

### **5.8.2 Deconvolution study of annealed NSQ samples of OSL at ET under the influence of beta doses.**

Within 0 to 0.4 seconds of optical stimulation at 160°C showed loss of OSL counts by average 89.75% as a rapid decay for 400°C annealed sample. These decrease in OSL counts slightly moved up by average 95.50% as a rapid decay in 600°C annealed sample, whereas the annealing treatment at 1000°C gave loss of OSL counts by average 40.58% as a rapid decay within 0 to 0.4seconds of stimulation (**Fig. 5.25**). In higher annealed samples, around 59.41% of OSL counts were decreased as a usual OSL decay. These usual OSL decay showed 72.31% contribution of slow components. These contributions systematically rise with annealing treatments. Also, the contribution of medium components of OSL decay increased with annealing temperature (**Table 5.15**). The photoionization cross section of medium and slow components of OSL decay curve found to be decreased with annealing temperature (**Table 5.16**).

While comparing deconvolution observations of OSL at ET between unannealed and annealed NSQ samples for beta doses interesting observations were brought out. The annealing of NSQ samples at 400°C and 600°C increased the average OSL loss percentage than average OSL loss percentage of unannealed samples as a rapid decay. But, the 1000°C annealed samples controlled the rapid loss of OSL percentages (**Fig. 5.16, Fig. 5.17 & Fig. 5.25**). Also, the lower annealed samples enhanced the contribution of medium components of OSL over the contribution of medium components of OSL of unannealed samples. Whereas, the growth of slower OSL components of higher annealed sample found to be more than the growth of slower OSL components of unannealed sample (**Table 5.12, Table 5.15**).The lower annealed samples increased the PIC of all components of OSL decay curves

over PIC of unannealed sample (**Table 5.13, Table 5.16**). However, higher annealed 1000°C samples decreases the PIC of all components of OSL decay curves over PIC of unannealed sample.

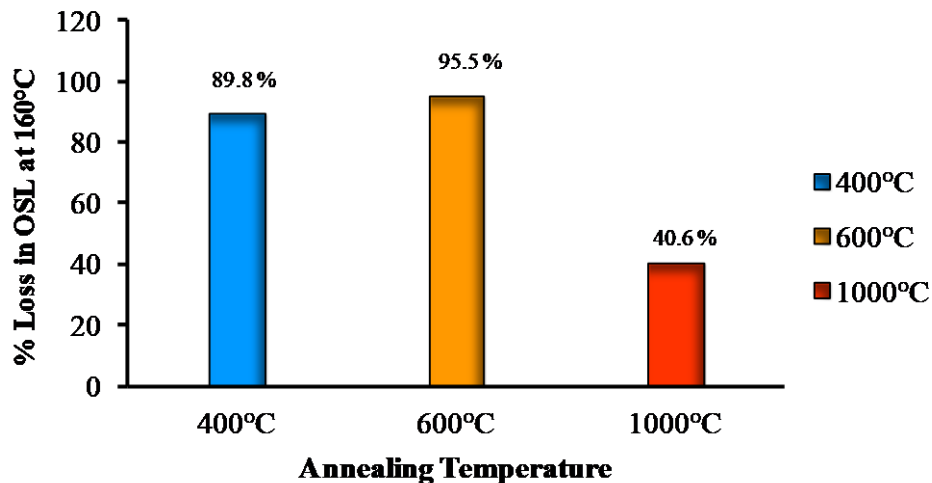


**Fig. 5.25** Observation for average percentage loss in OSL at 160°C within 0 to 0.4 seconds stimulation time for NSQ samples annealed at 400°C, 600°C and 1000°C.

### 5.9 OSL at ET-DRC study of NSQ samples.

The characteristics of OSL dose response under stimulation at 160°C was represented by the log (OSL-Intensity) versus log (Dose) scale. In this section, the OSL-DRC for pre-irradiated, annealed and unannealed NSQ samples at 160°C stimulation temperature was being considered.

#### 5.9.1 OSL at ET-DRC study of unannealed NSQ samples.

To understand the OSL sensitivity response of the sample with applied beta doses, the OSL decay curves were recorded at 160°C stimulation temperature. The unannealed samples exhibited systematic growth in OSL intensity from 4569.8counts to 433981.6counts under influence of 15.76Gy, 48.03Gy, 81.43Gy and 120.83Gy beta doses. Further rise in beta doses, the variations in OSL intensity were observed in the sample. In this part of the work, the slope value ( $k$ ) of OSL dose response is found to be more than one and hence it is pointed out as super-linear characteristics of OSL dose response for unannealed sample (**Table 5.18**).

**Table 5.18** Observations for OSL-DRC (at 160°C) of Unannealed, 400°C, 600°C and 1000°C annealed NSQ samples for (15.76Gy-199.6Gy) beta dose.

Sr. No.	Sample description	Slope (k)	Nature of Dose Response Curve
1	Un-annealed	1.006	Supra-linear
2	400°C Annealed	1.265	Supra-linear
3	600°C Annealed	0.791	Sub-linear
4	1000°C Annealed	0.767	Sub-linear

### 5.9.2 OSL at ET-DRC study of annealed NSQ samples.

The effect of annealing temperatures on OSL-DRC curves were studied under influence of beta doses. The nature of OSL-DRC curve was also determined by the calculating  $k$  value, which is related to the slope of the DRC. It was observed that 400°C annealed sample showed systematic growth of OSL counts and represented super-linear nature of dose response curve. However, higher annealed samples showed sub-linear nature of OSL dose response curve (**Table 5.18**). The higher annealed sample followed by beta doses changed super-linear to sub-linear nature of OSL dose response curve.

The lower annealing temperatures helped to enhance OSL strength in unannealed samples than higher annealing temperature. Either unannealed samples or 400°C annealed samples showed super-linear nature of OSL dose response curve. But the NSQ samples annealed at 600°C and 1000°C demonstrated sub-linear nature of OSL dose response curve (**Table 5.18**).

The annealing treatments offered significant strength of OSL counts than unannealed samples. Also, it was pointed out that the change of super-linear nature of OSL dose response of unannealed sample into sub-linear nature of dose response curves with thermal treatment.

### 5.10 Comparative study of deconvolution of OSL at RT and OSL at ET of NSQ samples.

Comparative studies on deconvolution of OSL of NSQ samples at room temperature and at 160°C had been carried out under identical annealing temperatures and beta radiation doses effects. These studies will reveal integrated effect of stimulation temperatures on OSL components, intensity and OSL dose response nature of the curves.

The optical stimulation at 160°C gave lower OSL strength compared to the optical stimulation at room temperature for pre-irradiated unannealed samples. The optical stimulation at 160°C for thermally treated samples followed by beta radiations, supported increase of the strength of OSL counts over the optical stimulation at room temperature (**Fig. 5.16, Fig. 5.25**).

During 0 to 0.4 seconds stimulation time, the optical stimulation at 160°C showed average OSL loss of 81.31% compared to average OSL loss of 78.21% as a rapid OSL decay in optical stimulation at room temperature. It suggested that stimulation at 160°C increased the loss of UFC components by average of 3% than loss of UFC at room temperature. It clearly indicates that suggested stimulation temperature is not much effective. In other words, the optical stimulation at 160°C exhibited a lesser amount of loss of OSL counts as a usual OSL decay.

Also, during 0.4 to 100 seconds stimulation time it helped to increase effective contribution of fast and medium components of OSL. But, the PIC of fast component and medium components of OSL remained much effective (**Table 5.13 & Table 5.14**).

The annealing temperatures for NSQ samples at 400°C and 600°C believed to support increase the loss of UFC during optical stimulation at 160°C over OSL at room temperature. Further, optical stimulation at 160°C increased the contribution of slower components of OSL by diminishing the contribution of medium components of OSL under influence of annealing temperatures. The PIC of slower of components of OSL was found to be more effective at stimulation of 160°C under the influence of annealing temperatures (**Fig. 5.17, Fig. 5.25**), (**Table 5.15, Table 5.16**).

### 5.11 Electron Spin Resonance Analysis

Benny P et al., Ranjbar et al. and Pires E et al. worked on ESR study of observed defect centers which was correlated with the TL and OSL outputs<sup>11,38,39</sup>. In present study, the contribution of traps in TL and OSL outputs were correlated by ESR output of prepared unannealed and annealed NSQ samples followed by different beta dose. These outcomes confirm the findings of TL-OSL correlation for different protocols of studies with significant outcomes.

ESR spectra of unannealed and different annealed NSQ samples followed by 55Gy and 200Gy beta doses are shown in **Fig. 5.26, Fig. 5.27, Fig. 5.28, Fig. 5.29, Fig. 5.30, Fig. 5.31, Fig. 5.32 & Fig. 5.33**. The ESR spectra for unannealed sample irradiated with 55 Gy showed ESR signal at g-value 2.0003 and 1.9956. The ESR signal was observed at g-value 2.0003 has been assigned to  $E_1'$  center on the basis of g-value<sup>40 41</sup> and the ESR signal at g-value 1.9956 has been allocated to  $E_1'$ -centers perturbed by a  $Ge^{4+}$  substituting for  $Si^{4+}$  in the  $SiO_4$  tetrahedron on the basis of g-value<sup>7</sup>. For 400°C annealed sample irradiated with 55 Gy exhibited ESR signal at g-value 2.0003 and 1.9959. Where, ESR signal at g-value 2.0003 has been assigned to  $E_1'$  center<sup>40,41</sup> while g-value 1.9959 has been allocated to  $E_1'$ -centers perturbed by a  $Ge^{4+}$  substituting for  $Si^{4+}$  in the  $SiO_4$  tetrahedron on the basis of g-value<sup>7</sup>. Peak to peak intensity of  $E_1'$  center in ESR spectra of 400°C annealed sample irradiated with 55 Gy was decreased as compared to ESR spectra of unannealed sample.  $E_1'$  center (g-value 1.9996, 1.9953)<sup>11</sup> in ESR spectra of 600°C annealed sample for 200Gy dose was believed to be started to decay with the development of Ge center with weak strength. The ESR spectra of 1000°C annealed sample for both 55Gy and 200Gy dose radiation clearly demonstrated the decay of  $E_1'$  center (g-value 1.9999, 1.9996)<sup>3</sup> with the development of Ge centers (1.9972, 1.9953)<sup>13</sup>. The ESR results might be reported that existence of  $E_1'$  center either in unannealed or annealed samples followed by dose. It is responsible to significant contribution of 110°C TL glow peaks under influence of beta dose, annealing treatments (400°C and 600°C) and optical bleaching at room temperature. Also, it is attributed to rapid decay within 0-0.4sec of stimulation time as an unusual part OSL decay curve.

The higher annealed samples followed beta doses and bleaching temperature show (i) the contribution from usual pattern of decay curve increases within 0.4 to 100sec (ii) the development of medium and slow components of OSL decay by diminishing of UFC (iii) thermal stability within 220°-230°C TL glow peaks. It is due to development of Ge center by decreasing the contribution of shallow traps corresponding to  $E_1'$  center (Table 5.19).



Fig. 5.26 ESR spectra for unannealed NSQ sample irradiated with 55Gy.

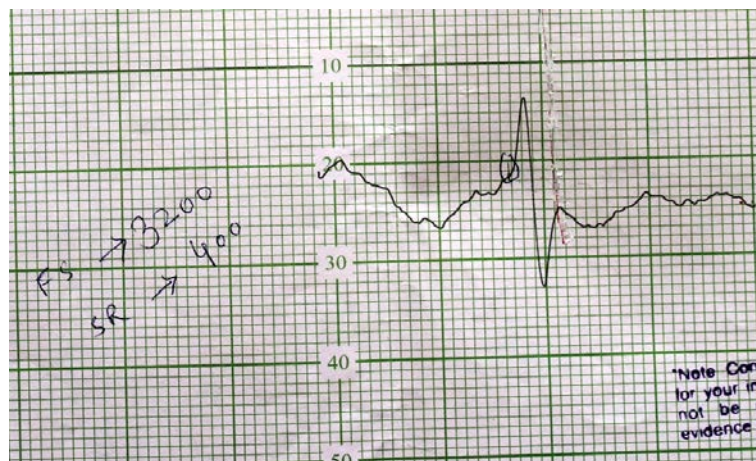


Fig. 5.27 ESR spectra for 400°C annealed NSQ sample irradiated with 55Gy.



**Fig. 5.28** ESR spectra for 600°C annealed NSQ sample irradiated with 55Gy.



**Fig. 5.29** ESR spectra for 1000°C annealed NSQ sample irradiated with 55Gy.

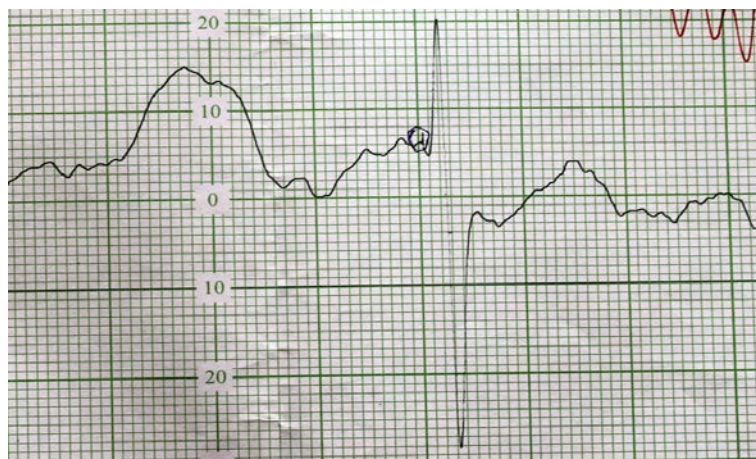


**Fig. 5.30** ESR spectra for unannealed NSQ sample irradiated with 200Gy.

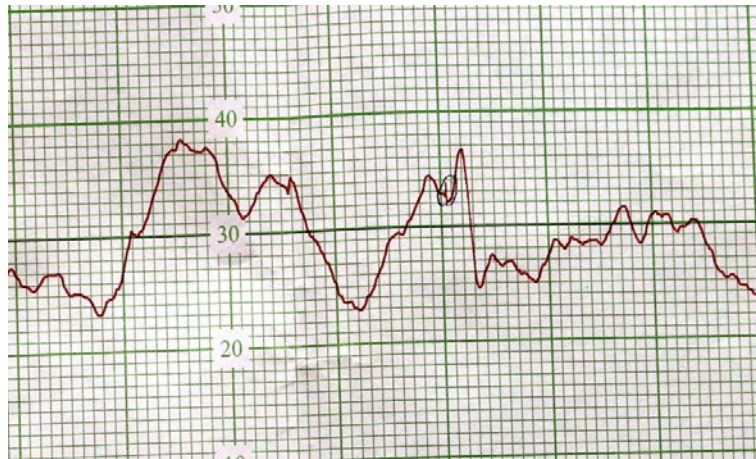


**Fig. 5.31** ESR spectra for 400°C annealed NSQ sample irradiated with 200Gy.

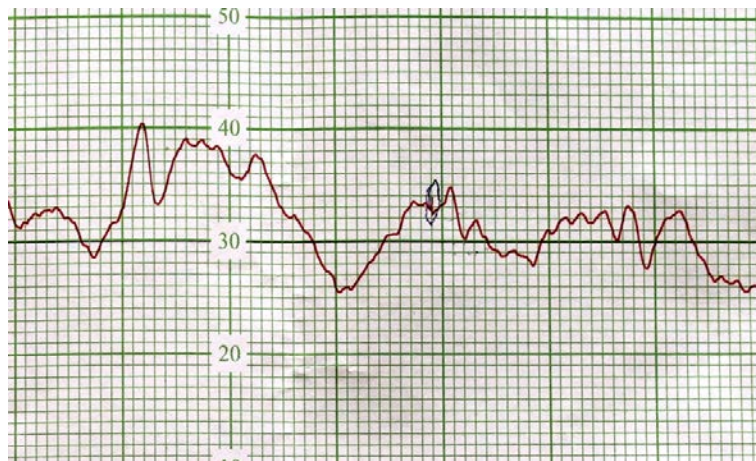


**Fig. 5.32** ESR spectra for 600°C annealed NSQ sample irradiated with 200Gy.

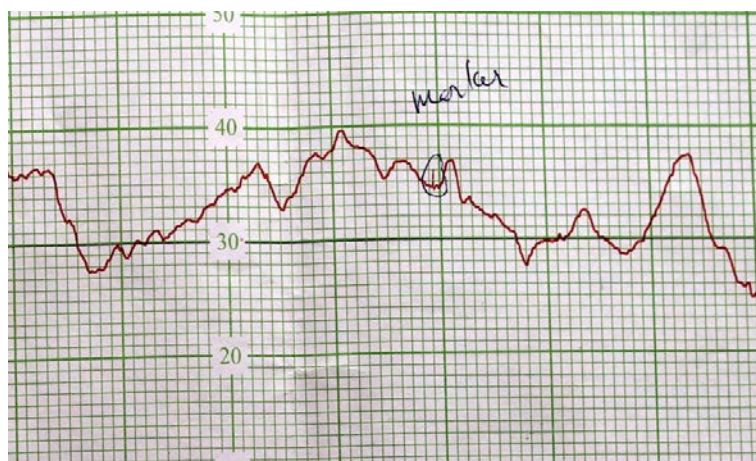


**Fig. 5.33** ESR spectra for 1000°C annealed NSQ sample irradiated with 200Gy.

**Table 5.19** Summary and outcomes of ESR study of annealed and un-annealed NSQ sample irradiated with different beta radiation dose.

Sr. No.	Thermal Treatment	Beta radiation Dose (Gy)	g-value	Possible Outcomes
1	Unannealed	55	2.0003	E <sub>1</sub> '-center is present
			1.9956	Center assigned to E <sub>1</sub> '-centers perturbed by a Ge <sup>4+</sup> substituting for Si <sup>4+</sup> in the SiO <sub>4</sub> tetrahedron
2	Annealed at 400°C	55	2.0003	E <sub>1</sub> ' center is present
			1.9959	Center assigned to E <sub>1</sub> '-centers perturbed by a Ge <sup>4+</sup> substituting for Si <sup>4+</sup> in the SiO <sub>4</sub> tetrahedron
3	Annealed at 600°C	55	2.0002	E <sub>1</sub> ' center is present
			2.0003	E <sub>1</sub> ' center is present
4	Annealed at 1000°C	55	1.9978	Decay in E <sub>1</sub> '-center and development of Ge-center
			1.9953	Decay in E <sub>1</sub> '-center and development of Ge-center
5	Unannealed	200	2.0003	E <sub>1</sub> '-centers is present
			1.9947	Center assigned to E <sub>1</sub> '-centers perturbed by a Ge <sup>4+</sup> substituting for Si <sup>4+</sup> in the SiO <sub>4</sub> tetrahedron
6	Annealed at 400°C	200	2.0003	E <sub>1</sub> '-center is present
			1.9966	Ge-center is present
7	Annealed at 600°C	200	1.9996	Decay in E <sub>1</sub> '-center and development of Ge-center
			1.9953	Decay in E <sub>1</sub> '-center and development of Ge-center
8	Annealed at 1000°C	200	1.9999	Decay in E <sub>1</sub> '-center and development of Ge-center
			1.9972	Decay in E <sub>1</sub> '-center and development of Ge-center

## Reference

- 1 Bøtter-Jensen, L. Development of optically stimulated luminescence techniques using natural minerals and ceramics, and their application to retrospective dosimetry. (2000).
- 2 McKeever, S. Thermoluminescence in quartz and silica. *Radiation Protection Dosimetry* **8**, 81-98 (1984).
- 3 Toktamiş, H. & Yazici, A. N. Effects of annealing on thermoluminescence peak positions and trap depths of synthetic and natural quartz by means of the various heating rate method. *Chinese Physics Letters* **29**, 087802 (2012).
- 4 Polymeris, G., Kitis, G. & Pagonis, V. The effects of annealing and irradiation on the sensitivity and superlinearity properties of the 110 C thermoluminescence peak of quartz. *Radiation Measurements* **41**, 554-564 (2006).
- 5 Yang, X. & McKeever, S. The pre-dose effect in crystalline quartz. *Journal of Physics D: Applied Physics* **23**, 237 (1990).
- 6 Chen, R., Abu-Rayya, M. & Kristianpoller, N. Sensitization of thermoluminescence in synthetic quartz—heat treatment and radiation effects. *Journal of luminescence* **48**, 833-837 (1991).
- 7 Carvalho Jr, Á. B. d., Guzzo, P. L., Sullasi, H. L. & Khoury, H. J. Effect of particle size in the TL response of natural quartz sensitized by high dose of gamma radiation and heat-treatments. *Materials Research* **13**, 265-271 (2010).
- 8 Cruz-Vázquez, C., Burruel-Ibarra, S., Grijalva-Monteverde, H., Chernov, V. & Bernal, R. Thermally and optically stimulated luminescence of new ZnO nanophosphors exposed to beta particle irradiation. *Radiation Effects & Defects in Solids* **162**, 737-743 (2007).
- 9 Ahmed, N. Investigation of Luminescence Characteristics of Some Synthetic Nano phosphors and Possibility of Application in Mixed Field Radiation Detection. (2013).
- 10 Shafiqah, A. S., Amin, Y., Nor, R. M. & Bradley, D. Effect of particle size on the thermoluminescence (TL) response of silica nanoparticles. *Radiation Physics and Chemistry* **117**, 102-107 (2015).
- 11 Benny, P., Rao, T. G. & Bhatt, B. The  $E_1'$ -centre and its role in TL sensitization in quartz. *Radiation measurements* **35**, 369-373 (2002).
- 12 Koul, D. 110° C thermoluminescence glow peak of quartz—A brief review. *Pramana* **71**, 1209-1229 (2008).
- 13 Kale, Y. D. Optically stimulated luminescence of synthetic quartz for different protocols and their correlation with thermoluminescence. (2005).
- 14 Spooner, N., Prescott, J. & Hutton, J. The effect of illumination wavelength on the bleaching of the thermoluminescence (TL) of quartz. *Quaternary Science Reviews* **7**, 325-329 (1988).
- 15 Morris, M. & McKeever, S. Optical bleaching studies of quartz. *Radiation measurements* **23**, 323-327 (1994).
- 16 McKeever, S. Models for optical bleaching of thermoluminescence in sediments. *Radiation Measurements* **23**, 267-275 (1994).
- 17 McKeever, S. & Chen, R. Luminescence models. *Radiation Measurements* **27**, 625-661 (1997).
- 18 Woda, C. *et al.* Potential and limitations of the 210 C TL peak in quartz for retrospective dosimetry. *Radiation Measurements* **46**, 485-493 (2011).
- 19 Kale, Y. & Gandhi, Y. Effect of temperature of optical stimulation on thermoluminescence peak of synthetic quartz. (2009).
- 20 Bøtter-Jensen, L., McKeever, S. W. & Wintle, A. G. *Optically stimulated luminescence dosimetry*. (Elsevier, 2003).
- 21 Pagonis, V., Chen, R. & Lawless, J. L. Superlinear dose response of thermoluminescence (TL) and optically stimulated luminescence (OSL) signals in luminescence materials: An analytical approach. *Journal of Luminescence* **132**, 1446-1455 (2012).
- 22 Lawless, J., Chen, R. & Pagonis, V. Sublinear dose dependence of thermoluminescence and optically stimulated luminescence prior to the approach to saturation level. *Radiation Measurements* **44**, 606-610 (2009).
- 23 Chen, R., Yang, X. & McKeever, S. The strongly superlinear dose dependence of thermoluminescence in synthetic quartz. *Journal of Physics D: Applied Physics* **21**, 1452 (1988).
- 24 Charitidis, C., Kitis, G., Furetta, C. & Charalambous, S. Superlinearity of synthetic quartz: dependence on pre-dose. *Radiation protection dosimetry* **84**, 95-98 (1999).

- 25 Charitidis, C., Kitis, G., Furetta, C. & Charalambous, S. Superlinearity of synthetic quartz: dependence on the firing temperature. *Nuclear Instruments and Methods in Physics Research Section B: Beam Interactions with Materials and Atoms* **168**, 404-410 (2000).
- 26 Silva, E. C., Ferraz, W. B. & Faria, L. O. Investigation of the thermoluminescent properties of nanosized Alpha-Al<sub>2</sub>O<sub>3</sub> doped with carbon for application in digital radiography. (2013).
- 27 Bhatt, B. C. Thermoluminescence, optically stimulated luminescence and radiophotoluminescence dosimetry: An overall perspective. *Radiation Protection and Environment* **34**, 6 (2011).
- 28 Kale, Y., Gandhi, Y. & Gartia, R. Dose-dependent optically stimulated luminescence of synthetic quartz at room temperature. *Journal of Luminescence* **128**, 1913-1916 (2008).
- 29 McKeever, S., Bøtter-Jensen, L., Larsen, N. A. & Duller, G. Temperature dependence of OSL decay curves: experimental and theoretical aspects. *Radiation Measurements* **27**, 161-170 (1997).
- 30 Preusser, F. *et al.* Quartz as a natural luminescence dosimeter. *Earth-Science Reviews* **97**, 184-214 (2009).
- 31 Bøtter-Jensen, L., Jungner, H. & Mejdahl, V. Recent developments of OSL techniques for dating quartz and feldspars. *Radiation Protection Dosimetry* **47**, 643-648 (1993).
- 32 Kale, Y. & Gandhi, Y. Influence of pre-measurement thermal treatment on OSL of synthetic quartz measured at room temperature. *Journal of Luminescence* **128**, 499-503 (2008).
- 33 Mandlik, N. *et al.* Study of TL and optically stimulated luminescence of K<sub>2</sub>Ca<sub>2</sub>(SO<sub>4</sub>)<sub>3</sub>: Cu nanophosphor for radiation dosimetry. *Journal of Luminescence* **146**, 128-132 (2014).
- 34 Kumar, M. & Datta, D. Limitations of conventional fitting methodology used for continuous wave optically stimulated luminescence (CWOSL) curves.
- 35 Bailey, R., Smith, B. & Rhodes, E. Partial bleaching and the decay form characteristics of quartz OSL. *Radiation Measurements* **27**, 123-136 (1997).
- 36 Banerjee, D. Supralinearity and sensitivity changes in optically stimulated luminescence of annealed quartz. *Radiation Measurements* **33**, 47-57 (2001).
- 37 Murray, A. & Wintle, A. Factors controlling the shape of the OSL decay curve in quartz. *Radiation Measurements* **29**, 65-79 (1998).
- 38 Ranjbar, A., Durrani, S. & Randle, K. Electron spin resonance and thermoluminescence in powder form of clear fused quartz: effects of grinding. *Radiation measurements* **30**, 73-81 (1999).
- 39 Pires, E. *et al.* TL, OSL and ESR properties of nanostructured KAlSi<sub>3</sub>O<sub>8</sub>: Mn Glass. *Radiation Measurements* **46**, 1492-1495 (2011).
- 40 Jani, M., Bossoli, R. & Halliburton, L. Further characterization of the E<sub>1</sub>' center in crystalline SiO<sub>2</sub>. *Physical Review B* **27**, 2285 (1983).
- 41 Benny, P., Sanjeev, N., Rao, T. G. & Bhatt, B. Gamma ray induced sensitization of 110° C TL peak in quartz separated from sand. *Radiation measurements* **32**, 247-252 (2000).